The DEAD-box RNA helicases RhlE2 is a global regulator of *Pseudomonas aeruginosa* lifestyle and pathogenesis

Stéphane Hausmann[1#], Diego Gonzalez[2#], Johan Geiser[1] and Martina Valentini[1]*

[1] Department of Microbiology and Molecular Medicine, CMU, Faculty of Medicine, University of Geneva, Geneva, Switzerland.

[2] Laboratory of Microbiology, Institute of Biology, Faculty of Sciences, University of Neuchâtel, Neuchâtel, Switzerland.

#: these authors contributed equally to the work.

* To whom correspondence should be addressed. e-mail: Martina.Valentini@unige.ch

Abstract

The RhlE DEAD-box RNA helicase protein family is widespread among Proteobacteria, but it is the least understood due to the lack of a clear biological function. Here, we study the two RhlE homologs present in the opportunistic pathogen *Pseudomonas aeruginosa*. RhlE1 and RhlE2 diverged during *P. aeruginosa* evolution; our data indicate that this resulted in a non-redundant biological role, a distinct molecular action and an enzymatic activity differentially stimulated by RNA. Whereas RhlE1 is specifically necessary for bacteria growth in cold, we show that RhlE2 acts as global post-transcriptional regulator, affecting the level of hundreds of cellular transcripts and multiple functionalities indispensable not only for *P. aeruginosa* environmental adaptation, but also for its virulence. The global action of RhlE2 relies on a unique C-terminal extension, which establishes an RNA-dependent interaction with the RNase E endonuclease and the cellular RNA degradation machinery.

Introduction

DEAD-box RNA helicases are RNA-binding proteins that upon ATP binding and hydrolysis remodel RNA structure and RNA–protein complexes (1). DEAD-box RNA helicases are found in all three domains of life, as well as in some viruses, and they are identified on the basis of highly conserved amino acid motifs within the catalytic core, "D-E-A-D" being one of those motifs (2,3). Besides the conserved catalytic region, they possess variable N- and C-terminal extensions that can regulate the core catalytic activity or coordinate interactions with RNA molecules or proteins (4-7). The *Escherichia coli* DbpA RNA helicase, for example, contains an RNA-binding domain (RBD) at the C-terminus, which is responsible for a specific and tight binding to hairpin 92 of 23S ribosomal RNA (8).

From bacteria to humans, DEAD-box RNA helicases are involved in maintaining a correct basal RNA metabolism, by controlling mRNA translation, RNA degradation and ribosome biogenesis (1). In bacteria, though, DEAD-box RNA helicases do not perform only housekeeping functions, but can also regulate their environmental adaptation, host colonization and, in case of pathogens, infectious processes (9-11).

Bacterial DEAD-box RNA helicases can be classified into to three major phylogenetic groups, that are distinguished by the presence of DbpA-RBD: DbpA RBD-containing proteins, DbpA RBD-lacking proteins and RhlE-like proteins (12). The RhlE-like RNA helicases, which are named from the *E. coli* DEAD-box RNA helicase belonging to this group, seem to have originated from a duplication of a DbpA-RBD lacking protein in a Proteobacterial ancestor and have successively expanded in this phylum, where they can be present in several copies per genome (12). The role and molecular action of RhlE-like proteins are not understood, and they vary across species. No phenotypic defect linked to *rhlE* deletion has been described in *E. coli*, *Pseudomonas syringae* LZ4W and *Mycobacterium tuberculosis*, while in *Yersinia pseudotuberculosis* and *Caulobacter crescentus* deletion of *rhlE* affects cold acclimation (13-18). In *E. coli*, RhlE seems to liaise with the SrmB and CsdA RNA helicases during ribosome biogenesis, although the exact molecular action is not yet deciphered, and to interact with the RNase E endonuclease for RNA degradation, even if the conditions in which the interaction occurs in vivo are unclear (19,20). In *P. syringae* LZ4W, *M. tuberculosis* and *C. crescentus*, RhlE is

53 described as a core component of the cellular RNA degradosome machinery, hence involved in RNA
54 degradation (13,17,18).
55 In the present study, we investigate the role of RhlE proteins in the Gram-negative bacterium
56 *Pseudomonas aeruginosa*. The bacterium has a remarkable distribution across multiple ecological
57 niches, including a wide variety of hosts (21-23). In humans, *P. aeruginosa* infections pose a significant
58 life threat to immunocompromised and immunodeficient persons, intensive care patients, patients with
59 cystic fibrosis or other forms of bronchiectasis and chronic obstructive pulmonary diseases (24-28). As
60 opportunistic pathogen, *P. aeruginosa* possesses a remarkable virulence plasticity, being able to
61 colonize different type of organs and modify its virulence strategy and physiology in response to the
62 host context (29). Scarce information exists on *P. aeruginosa* DEAD-box RNA helicase genes and their
63 role on the regulating the bacterium versatility (30). In addition, we noticed that the genome of *P.*
64 *aeruginosa* encodes two *rhlE* genes: PA3950 (*rhlE1*) and PA0428 (*rhlE2*), making the bacterium an
65 ideal model to assess any redundancy and neofunctionalization among duplicated RhlE proteins.
66 Here, we reveal that both RhlE1 and RhlE2 are important for *P. aeruginosa* cold adaptation, but *rhlE2*
67 mutation results in a broader pleiotropic effect on motility, biofilm formation and virulence. We assess
68 RhlE1 and RhlE2 RNA preferences in vitro and we identify the RhlE2 regulon in vivo. Moreover, we
69 define a model of RhlE2 mechanism of action whereby RhlE2 affects RNA stability via an unusual
70 interaction with RNase E, which is dependent on RNA and RhlE2 C-terminal extension. Finally, we
71 discuss the phylogenetic diversity of RhlE proteins by comparing *P. aeruginosa* RhlE proteins with
72 previously characterized RhlE proteins in other Proteobacteria.
73

74 ## Results

75 ### ***Pseudomonas aeruginosa* encodes two RhlE-like RNA helicases with different origin and features**

76 The RhlE-like group RNA helicases is widespread in Proteobacteria, with sometimes several homologs
77 present in a single genome (9,12). In most *Pseudomonas* species two RhlE homologs are found,
78 belonging to two different terminal branches of the RhlE phylogenetic tree that groups eight main clades
79 (**Fig 1A** and **S1**). In *P. aeruginosa* PAO1 genome, two genes encode for RhlE-like proteins, PA3950

80 (RhlE1) and PA0428 (RhlE2), having 51% and 43% sequence identity to the *E. coli* RhlE, respectively
81 (**Fig 1B**). RhlE1 is found on a branch represented mostly in environmental bacteria, including *Vibrio,*
82 *Shewanella, Legionella* or *Azotobacter* species; while the clade where the RhlE2 belongs includes many
83 *Pseudomonas* genus (**Fig S1**). Alignment of representative RhlE homologs shows that the canonical
84 RecA1 and RecA2 RNA helicase domains are conserved, including the ten short motifs typical of
85 DEAD-box RNA helicases, while high sequence divergence is present at the C-terminus of the proteins
86 (**Fig S2**). Clustering of the C-terminal extension among RhlE homologs does not show any global
87 pattern; it is therefore likely that C-terminal regions are clade-specific and fast evolving. In *P.*
88 *aeruginosa*, RhlE1 possesses a short CTE that contains a stretch of lysine-rich amino acids, while RhlE2
89 possess the longest CTE among RhlE-like proteins that includes a stretch of ~50 amino acids rich in
90 glycine-glutamate (**Fig S3**).
91
92 **RhlE1 and RhlE2 are both necessary for *P. aeruginosa* cold adaptation, but are not redundant**
93 Cold sensitivity is a phenotype that has been previously associated to inactivation of RNA helicase
94 genes and in particular to *rhlE* inactivation in *Y. pseudotuberculosis* and *C. crescentus* (9,13,14). To
95 investigate the role of RhlE homologs in *P. aeruginosa*, we constructed single *rhlE1* and *rhlE2* deleted
96 strains as well as a double Δ*rhlE1*Δ*rhlE2* mutant and we tested growth on cold. Specifically, we
97 evaluated the growth properties of the deletion strains compared to the wild type by spotting serial
98 dilutions of cells (from liquid cultures adjusted to an OD600 of 1.0) on LB agar medium and incubating
99 plates at 37°C and 16°C. At 37°C all mutants displayed similar growth as the wild type strain, as shown
100 by CFU counting of serial dilutions (**Fig 2A**), as well as by OD measurements of liquid cultures at
101 different time points (**Fig S4**). By contrast, at 16°C, deletion of *rhlE1* or *rhlE2* resulted in a growth
102 defect, which was further increased in the Δ*rhlE1*Δ*rhlE2* mutant (**Fig 2B**). Both RhlE1 and RhlE2 are
103 shown to be important for cold adaptation, but while loss of *rhlE1* produced a severe growth delay, loss
104 of *rhlE2* was only slightly deleterious. We then tested if the functions of RhlE1 and RhlE2 overlap
105 during cold growth, by preforming complementation experiments. To do so, we employed the mini-
106 Tn7 system to insert into the chromosomal Tn7 attachment site of Δ*rhlE1*, Δ*rhlE2* or Δ*rhlE1*Δ*rhlE2*

107 mutants a copy of *rhlE1* or *rhlE2* gene under the control of an arabinose-inducible promoter. As the
108 genes carried by the mini-Tn7 constructs were cloned in frame with a N-terminal 3xFLAG epitope, we
109 could verify their expression levels by Western blot, which were comparable (**Fig S5**). As shown in **Fig**
110 **2C**, growth of the *rhlE1* mutant at 16°C could be restored to wild type levels by the insertion of the
111 mini-Tn7_3xFLAG-RhlE1 (::3xFLAG-E1) construct, likewise for the complementation of *rhlE2*
112 mutant by the mini-Tn7_3xFLAG-RhlE2 (::3xFLAG-E2). However, it was not possible to fully restore
113 the growth at 16°C of the Δ*rhlE1*Δ*rhlE2* mutant by reintroduction *in trans* of only one *rhlE* gene **(Fig**
114 **2C)**, nor to complement the phenotype of the *rhlE1* mutant by 3xFLAG-E2 and vice versa (**Fig S6**).
115 Altogether, these data provide evidence that RhlE1 and RhlE2 perform unique and specific regulatory
116 actions during growth on cold, as they are not redundant and do not cross-complement each other.
117
118 **RhlE2 is a global lifestyle regulator in *P. aeruginosa***
119 Some bacterial RNA helicases have been shown to regulate other cell functions besides cold growth
120 and to be involved in environmental adaptation or even pathogenicity (9,11). Thus, we tested whether
121 RhlE1 and RhlE2 could also impact medically relevant physiology and behaviour of *P. aeruginosa*. We
122 first tested the *rhlE* mutant strains motility in liquid and on surfaces (**Fig 3A**), then their capacity to
123 form early and mature biofilms (**Fig 3B**). Having ruled out a growth defect of the strains at 37°C, all
124 the experiments were carried at this temperature. Interestingly, the Δ*rhlE2* mutant was strongly affected
125 on all these traits, being less motile (20, 2.5- and 15-fold reduction of swimming, twitching and
126 swarming, respectively) and significantly impaired in biofilm formation (3- and 1.5-fold decrease of
127 early and mature biofilm, respectively) when compared to the wild type strain. By contrast, deletion of
128 *rhlE1* did not results in significant differences compared to wild type, while the Δ*rhlE1*Δ*rhlE2* mutant
129 phenotype didn't differ from the Δ*rhlE2* strain. Altogether, these results revealed that RhlE2 affects
130 several functionalities and cellular processes in *P. aeruginosa*, thus acting as global lifestyle regulator;
131 while RhlE1 role is specific to cold adaptation. This conclusion is validated by the observation that
132 complementation of the Δ*rhlE1*Δ*rhlE2* mutant with 3xFLAG-E2 was able to fully restore swarming
133 motility to wild type levels, whereas the Tn7 construct carrying *rhlE1* failed (**Fig 3C**). Finally, the lack

134 of a phenotype linked to a *rhlE1* deletion even in absence of *rhlE2* indicates that no buffering exists
135 among these two RNA helicases **(Fig. 3A and 3B).**
136
137 **RNA sequencing analysis reveals the importance of RhlE2 for *P. aeruginosa* virulence**
138 To examine further the role of RhlE2 in *P. aeruginosa*, we compared the transcriptome of *rhlE2* deleted
139 strains in the wild type or in the Δ*rhlE1* background, by performing RNA-sequencing. As experimental
140 condition, we choose to investigate the role of RhlE2 in swarming cells (**Fig 4A**). Swarming motility is
141 a coordinated movement of a bacterial population on semi-solid surfaces (0.5 to 0.7% agar), which is
142 mediated by flagella rotation and surfactants secretion (31). Importantly, *P. aeruginosa* swarming cells
143 possess a physiological state which is highly relevant to the bacterium pathogenicity as they express
144 virulence factors, they perform epithelial surfaces colonization and are associated to the establishment
145 of lungs infection through biofilm formation (32,33). Approximately 15% of the transcriptome was
146 significantly affected by *rhlE2* mutation when compared to wild type PAO1 (N=836 genes, *p*-value
147 <0.05, FC>2), of which 4% (N=228) of transcripts were up-regulated and 11% (N=608) down-regulated
148 (**Fig 4B**, **Table S1**). Differentially regulated genes were grouped into the corresponding KEGG
149 pathway: most significantly downregulated genes code for ribosomal proteins, metabolic pathways and
150 enzymes involved in the biosynthesis of secondary metabolites, while upregulated ones are linked to
151 xenobiotics biodegradation and metabolism (e.g. 4-fluorobenzoate, chlorocyclohexane and
152 chlorobenzene degradation, **Table S2**). Consistent with the phenotypic analysis, *rhlE1* deletion had not
153 significant impact on the cellular transcript levels neither in the wild type nor in the *rhlE2* mutant
154 background (**Fig 4B**). Next, we validated the transcriptome analysis by choosing a set of putative RhlE2
155 targets and examining their abundance by RT-qPCR in the Δ*rhlE1*, Δ*rhlE2* and Δ*rhlE1*Δ*rhlE2* mutants
156 as compared to the wild type, starting from cell grown under experimental conditions similar to those
157 used for the original RNA-sequencing analysis. The gene chosen have been previously shown to either
158 regulate swarming or being regulated in this condition, such as *roeA*, coding for a diguanylate cyclase
159 (34), *lhpF,* coding for the metabolic enzyme D-hydroxyproline dehydrogenase (35), the *lasB* elastase
160 (36) and the *pvdF* pyoverdine synthase (37) encoding genes, and finally the *rhlA* gene was chosen as

161 control (rhamnosyltransferase chain A) being unaffected by *rhlE2* mutation, but previously shown
162 necessary for swarming motility (38). In agreement with the RNA-seq data, *lasB* and *pvdF* mRNA
163 levels were, respectively, 10.25 and 10.41-fold down-regulated in the Δ*rhlE2* mutant when compared
164 to the wild type; while *roeA* and *lhpF* were, respectively, 3.98 and 8.94-fold up-regulated and *rhlA*
165 mRNA levels were unchanged (**Fig 4C**). To further validate the observation concerning regulation of
166 *lasB* expression, a transcriptional/translational *lasB'-'lacZ* fusion (39) was assayed for β-galactosidase
167 activity in the four strains, at different growth phases in NYB (**Fig 4D**). Expression of *lasB* is dependent
168 on cell-density and therefore maximal at stationary phase (40), the same trend was observed in all
169 mutants but in the Δ*rhlE2* and Δ*rhlE1*Δ*rhlE2* mutants the expression of the *lasB'-'lacZ* fusion was
170 reduced of ~2.5-fold in stationary phase, when compared to the wild type and Δ*rhlE1* strains.
171 Besides *lasB*, one interesting observation concerning the *rhlE2* mutant transcriptome was the significant
172 downregulation of various other genes encoding virulence factors (**Table S1**). To assess whether mRNA
173 levels regulation by RhlE2 also results in changes of virulence factor abundance, we measured in our
174 strains the extracellular levels of the LasB elastase and pyocyanin, a redox-active molecule inducing
175 oxidative stress in host cells (41). We found that the Δ*rhlE2* and Δ*rhlE1*Δ*rhlE2* mutants produced 2.6-
176 and 3.6-fold less elastase and 2,1- and 2.4-fold less pyocyanin than the wild type, respectively, while
177 the *rhlE1* deletion did not produce any significant difference (**Fig 5A-B**).
178
179 **RhlE2 affects *P. aeruginosa* virulence in *Galleria mellonella***
180 *Galleria mellonella* has become an important model to study bacterial pathogenesis (42). We used this
181 system to confirm that RhlE2 has indeed an important role during *P. aeruginosa* pathogenesis *in vivo*.
182 In agreement with data disclosed above, the Δ*rhlE2* and Δ*rhlE1*Δ*rhlE2* mutants displayed a significant
183 attenuation of virulence in the *G. mellonella* infection model. Indeed, at 24 hours post-infection the
184 mortality of larvae injected with either Δ*rhlE2* or Δ*rhlE1*Δ*rhlE2* reached less than 40%, while the
185 mortality rate of larvae challenged with wild type or Δ*rhlE1* strain was 80% (**Fig 5C**). Altogether, these
186 results indicate that RhlE2 controls, directly and/or indirectly, the expression of virulence or virulence-
187 related genes and is necessary for *P. aeruginosa* pathogenicity *in vivo*.

188

189 **RhlE1 and RhlE2 display an RNA-dependent ATPase activity in vitro**

190 To fuel their molecular actions, RNA helicases possess an ATP hydrolytic activity that is dependent on
191 RNA binding (2). To confirm this prediction, based on RhlE1 and RhlE2 sequence conservation, we
192 assess their enzymatic activity in vitro. The proteins were produced in *E. coli* as N-terminal His_{10}-Smt3-
193 tagged fusion and purified from a soluble extract by adsorption to nickel-agarose and elution with 250
194 mM imidazole (**Fig 6A**). As control, we also purified the RhlE1 and RhlE2 catalytic mutants, in which
195 the Lys51 of RhlE1 and RhlE2 within motif I (involved in ATP binding and hydrolysis) is replaced by
196 Ala, making the proteins inactive (43). As shown in **Fig 6B**, recombinant RhlE1 and RhlE2 catalyzed
197 the release of ^{32}Pi from [γ-^{32}P] ATP in the presence of poly(U) RNA and that the extent of ATP
198 hydrolysis was proportional to the protein concentration. From the slope of the titration curves, we
199 estimated that RhlE1 and RhlE2 hydrolyzed 0.0119 nmol and 0.0068 nmol ATP per ng of enzyme,
200 respectively, during the 15 min reaction. These values translate into a turnover number of 51 min^{-1} for
201 RhlE1 and 37 min^{-1} for RhlE2 indicating that both RhlE proteins have a similar ATPase activity in the
202 presence of poly(U) RNA. As expected for DEAD-box RNA helicases, both RhlE1 and RhlE2 catalyzed
203 no detectable ATP hydrolysis in absence of RNA (**Fig 6B**). Moreover, the ATPase activity of $RhlE1_{K51A}$
204 and $RhlE2_{K51A}$ mutants were less than 1% of the activity of the respective wild type enzyme stimulated
205 by poly(U) RNA (**Fig 6C**), validating that the observed RNA dependent phosphohydrolase activities of
206 wild type RhlE1 and RhlE2 are intrinsic to the recombinant proteins.

207

208 **Characterization of the RhlE1 and RhlE2 RNA preferences**

209 As the size of poly(U) RNA is heterogeneous (> 150 ribonucleotides), we examined the effect of RNA
210 length on the ATPase activity of RhlE1 and RhlE2 by using a set of polyribouridylic acid of defined
211 length (U10, U16, U25 and U41, respectively). We found that the extent of phosphate release by RhlE1
212 with U41, U25, U16, U10 RNA substrate were 73, 27, 16, and 6% of the activity with poly(U) RNA,
213 respectively, while the corresponding RhlE2 ATPase activity was 35, 12, 1 and <1 % (**Fig 6D**). This
214 result indicates that RhlE2 ATPase activity requires RNA oligomers of ≥ 25 nucleotides (nt), whereas

215 RhlE1 can still be activated by RNA oligomers shorter than 16 nt.

216 We next examined whether the RNA secondary structure can affect the ATPase activity of RhlE
217 proteins. Therefore, we used three different 41-mer RNA substrates: a single-strand RNA (ssRNA), a
218 stem loop of 8 base-pairs with a 9-Us extension both at the 5' and 3' end ($shRNA^{8bp}$), and a blunt-ended
219 stem-loop RNAs with 17 base pairs in the stem region ($shRNA^{17bp}$; see **Fig S7**). The phosphate release
220 by RhlE1 was similar between the three different RNA substrates, whereas the ATPase activity of
221 RhlE2 was increased 3-fold with $shRNA^{8bp}$ and 4-fold with a blunt-ended stem-loop RNA $shRNA^{8bp}$,
222 compared to single strand RNA (ssRNA), indicating that RNA structure affects significantly the
223 ATPase activity of RhlE2 but not of RhlE1 (**Fig 6E**). Besides, similar release of phosphate by RhlE1
224 and RhlE2 is observed with the two 41-mer U41 and ssRNA single-strand RNAs (5.7 nmol and 3.9
225 nmol Pi for RhlE1 and 1.8 nmol and 1.5 nmol Pi for RhlE2, respectively), confirming that *in vitro*
226 ATPase of DEAD-box helicases display poor RNA sequence specificity (44-46). We also examined the
227 stimulatory effect of naturally occurring long-structured RNAs, namely MS2 RNA and *E. coli* rRNA.
228 We found that MS2 RNA and *E. coli* rRNA are strong activators of RhlE2 ATPase activity than poly(U)
229 RNA, displaying respectively 172% and 153% of the activity measured with poly(U); whereas RhlE1
230 ATPase activity was 66% and 62% of the activity with poly(U), respectively (**Fig 6F**). Altogether, these
231 results strongly suggest that ATPase activity of RhlE1 and RhlE2 are differently stimulated depending
232 on the length and structure of the RNA.

233

234 **The ATPase activity of RhlE1 is necessary for cold adaptation while the RhlE2 ATPase activity**
235 **is sometimes dispensable**

236 Having validated that the replacement of the lysine by alanine in the motif I abolished the catalytic
237 activity of RhlE1 and RhlE2, we sought to determine if the observed catalytic activity of RhlE1 or
238 RhlE2 was necessary for their role *in vivo*. We constructed mini-Tn7 variants expressing the 3xFLAG-
239 $RhlE1_{K51A}$ or 3xFLAG-$RhlE2_{K51A}$ mutant and we assessed their capacity to complement the phenotypes
240 of the corresponding deleted strain. Expression of the RhlE1 catalytic mutant (3xFLAG-$E1_{K51A}$) was
241 not able to restore the growth at 16°C of the *rhlE1* mutant, while surprisingly the $RhlE2_{K51A}$ construct

242 (3xFLAG-E2$_{K51A}$) was able to sustain growth at 16°C of the Δ*rhlE2* mutant (**Fig 2D**). We checked that
243 growth of the Δ*rhlE2*::3xFLAG-E2$_{K51A}$ at 16°C was not the result of suppressor mutations by
244 resequencing the mini-Tn7 construct of the strain grown at 16°C as well as by assessing the growth of
245 the strain in absence of arabinose (i.e. not inducing RhlE2$_{K51A}$ expression). Instead, the swarming
246 motility of the Δ*rhlE2* mutant expressing 3xFLAG-E2$_{K51A}$ was similar to the Δ*rhlE2* mutant (**Fig 7A**).
247 We also used the *lasB'-'lacZ* fusion as proxy of RhlE2 regulatory activity, as it was downregulated in
248 the Δ*rhlE2* mutant (**Fig 4D**). Again, the expression of the fusion was similarly affected in the Δ*rhlE2*
249 mutant expressing RhlE2$_{K51A}$ as in the Δ*rhlE2* mutant, while the 3FLAGxRhlE2 construct was restoring
250 the expression of *lasB'-'lacZ* in the Δ*rhlE2* mutant to the wild type levels (**Fig S8**). In all these
251 conditions, unlike at 16°C, the catalytic activity of RhlE2 is essential for its regulatory action.
252
253 **RhlE2 interacts with the Ribonuclease E via RNA**
254 One possibility to explain the different RhlE1 and RhlE2 regulatory actions was that they interact with
255 different protein partners. To test this hypothesis, we probed RhlE1 and RhlE2 proteins interacting
256 partners by protein affinity assays (pull-downs) using *P. aeruginosa* Δ*rhlE1*::3xFLAG-RhlE1 and the
257 Δ*rhlE2*::3xFLAG-RhlE2 strains, respectively. Strains were grown at 37°C to an OD600 of ~1.5 in
258 presence of 0.02% of arabinose and the proteins were purified using anti-FLAG antibody resin (see
259 Material and Methods). The protein profile of the eluted fractions was first analysed by SDS page and
260 then by mass-spectrometry (**Fig 8A)**. As control, we used an Δ*rhlE2* strain expressing untagged RhlE2
261 (CN). Two bands appeared specifically in the elution profile of the 3xFLAG-RhlE2 construct, one at
262 ~80 kDa corresponding to 3xFLAG-RhlE2 and one additional band at ~140 kDa that was excised from
263 the gel and identified by mass-spectrometry as RNase E. On the other hand, no band other rather than
264 RhlE1 was visible in the elution of the 3xFLAG-RhlE1 pull-down (**Fig 8B**). To identify putative
265 partners that were not visible as clear bands in denaturing gels stained with Coomassie, the entire eluted
266 samples were further analysed by mass-spectrometry. Additional proteins were consistently enriched
267 more than 2-fold in the 3xFLAG-RhlE2 elution of three independent pull-down experiments when

268 compared to the negative control (**Fig 8C**). Interestingly, the three most enriched proteins in the
269 3xFLAG-RhlE2 sample were ribonucleases: RNase E, PNPase and RNase R; suggesting a role of RhlE2
270 in RNA processing and degradation. The fourth most enriched protein was the DnaK chaperone, which
271 appeared enriched as well in the 3xFLAG-RhlE1 sample.
272 Next, we wondered whether the observed RhlE2-protein interactions were direct protein-protein
273 interactions or interactions mediated by RNA. To address this question, additional 3xFLAG-RhlE2 pull-
274 downs were performed by pre-treating cells with RNase A. The enrichment of peptides corresponding
275 to RNase E, PNPase and RNase R was lost in the 3xFLAG-RhlE2 elution sample treated with RNase
276 A, when compared to the untreated sample, attaining background levels comparable to the negative
277 control; whereas peptides corresponding to DnaK were still present (**Fig 8C**). Thus, we conclude that
278 RNA is necessary to mediate or stabilize any interaction of RhlE2 with RNases.
279 To confirm the pull-down results obtained, we performed bacterial two-hybrid assays, which report on
280 protein interactions based on proximity of split T25-T18 adenylyl cyclase domains (47). Co-expression
281 of T25-*rhlE2* and T18-*rne*, *rne* encoding RNase E, restored the enzyme activity and resulted in red
282 colonies when cells were grown in Congo Red medium and in a significant increase of β-galactosidase
283 activity compared to controls (**Fig 8D**). In agreement with the pull-down assays, T25-RhlE1 interaction
284 with T18-RNase E was not detected. In addition, the K51A mutation did not affect interaction of RhlE2
285 with T18-RNase E. Finally, interaction of RhlE2 with RNase R and PNPase was not detected via
286 bacterial two-hybrid assays, indicating that these interactions probably occur indirectly via *P.*
287 *aeruginosa* RNase E (**Fig S9**).
288
289 **The CTEs of RhlE2 is necessary for interaction with RNase E and the protein function in vivo**
290 In some cases, the CTE of RNA helicases is necessary for their function in vivo, being involved in
291 mediating interaction with other proteins and/or in recognition of RNA targets (8,48,49). RhlE2
292 possesses a unique CTE that differs from RhlE1 and from other RhlE homologs investigated so far (**Fig**
293 **S2**). We asked whether the RhlE2 CTE was important for its biological function by constructing a mini-
294 Tn7 construct carrying 3xFLAG-RhlE2 truncated of its C-terminal region (3xFLAG-RhlE2$_{1-434}$) and

295 performing complementation assays with Δ*rhlE2*::3xFLAG-RhlE2$_{1-434}$ strain (**Fig S4**). Deletion of the
296 CTE RhlE2 resulted in the inability to restore all the phenotypes tested, *i.e.* growth at 16°C and
297 swarming motility as well as the inability to restore expression of the *lasB'-'lacZ* reporter fusion to wild
298 type levels (**Fig 2D and Fig 7**).
299 Then, the RhlE2-RNase E interaction was probed via pull-down assays in a Δ*rhlE2*::3xFLAG-RhlE2$_{1-}$
300 $_{434}$ strain and via co-expression of T25-RhlE2$_{1-434}$ and T18-RNase E followed by bacterial two-hybrid
301 assays. With pull-downs, we could show that the interaction with RNase E was lost (compare the level
302 of RNase E on Coomassie gel in **Fig 8A** and in **Fig 8B**). The analysis of the eluates by mass-
303 spectrometry still reveals the presence of some RNase E peptides (56 peptides in 3XFLAG-RhlE2$_{1-434}$
304 versus 74 peptides in 3XFLAG-RhlE2; **Fig 8C**). However, the results with the bacterial two hybrids
305 showed unambiguously the involvement of the RhlE2 CTE in RNase E binding in vivo (**Fig. 8D**).
306 Having shown that the unique CTE of RhlE2 was necessary to interact with RNase E, we next asked
307 whether the CTE was necessary for RhlE2 catalytic activity. To address this question, the RhlE2$_{1-434}$
308 mutant was expressed in *E. coli* with an N-terminal His$_{10}$-Smt3-tag and purified as described previously
309 for RhlE2 (**Fig 9A**). The recombinant RhlE2$_{1-434}$ was still able to catalyze the release of ^{32}Pi from [γ-
310 ^{32}P] ATP in the presence of poly(U) RNA and the extent of ATP hydrolysis was proportional to enzyme
311 concentration, with 56% of the ATP substrate was hydrolyzed in 15 minutes reaction at 100 ng/µl
312 RhlE2$_{1-434}$ (**Fig 9B**). A specific activity of 0.011 nmol of ATP hydrolyzed per ng of protein in 15 min
313 was calculated from the slope of the titration curve in the linear range. This value translates into a
314 turnover number of 46 min^{-1}, which is similar to the RhlE2 wild type turnover (51 min^{-1}, **Fig 6B**). The
315 observed RNA independent phosphohydrolase activity of RhlE2$_{1-434}$ is intrinsic to the recombinant
316 protein as insofar the ATPase activity of the RhlE2$_{K51A,1-434}$ mutant in the presence poly(U) RNA was
317 less than 1% of the activity of RhlE2$_{1-434}$ (**Fig 9C**). From these results, we conclude that the CTE of
318 RhlE2 (amino-acid 434 to 648) is necessary for the protein regulatory action in vivo and its interaction
319 with RNase E, while it is dispensable for its RNA-dependent ATPase activity in vitro.
320
321 **RhlE2 affects the stability of some cellular RNAs**

322 The RhlE2 interaction with RNase E suggests that RhlE2 could perform a role in cellular RNA decay
323 (50). In order to test this hypothesis, we assessed the half-life of some mRNAs in the wild type and
324 Δ*rhlE2* mutant (**Fig 10**). For the analysis, we selected transcripts whose abundance appeared to be either
325 down-regulated or up-regulated in our RNAseq analysis (**Fig 4**). The mRNA which were up-regulated
326 in the *rhlE2* mutant, like PA1897, PA2314 or PA2268, displayed a 1.5 to 3-fold increase of their half-
327 life compared to the wild type. On the other hand, the stability of *lasB*, a down-regulated mRNAs, do
328 not seem to be affected by *rhlE2* deletion, probably indicating an indirect regulation by RhlE2. In
329 agreement with this hypothesis, we observed a down-regulation of *lasB* expression in the Δ*rhlE2* mutant
330 also when we used a transcriptional *lasB-lacZ* fusion, reporting only on the activity of the *lasB* promoter
331 rather than the mRNA stability or translation rate (**Fig S9**).
332

333 **Discussion**

334 The molecular mechanisms leading to *P. aeruginosa* pathogenesis have been a blooming subject of
335 investigation over the past decades. Numerous toxins, virulence and virulence-associated factors have
336 been shown to be responsible for the variety of infections associated to the bacterium (51). Yet new
337 regulatory networks are still to find. In this paper, we report for the first time the role of a RhlE protein
338 in the regulation of *P. aeruginosa* pathogenesis.
339 This study was initially motivated by two observations based on a phylogenetic analysis of the RhlE
340 group of proteobacterial RNA helicases. First, genes encoding RhlE proteins have expanded in
341 Proteobacteria through duplication events, reaching up to six copies in *Shewanella pealeana* ATCC
342 700345 (12), redundancy and sub-functionalization among RhlE proteins had not been investigated.
343 Second, RhlE homologs possess different and fast evolving C-terminal extensions. Whether variability
344 confers a different function to RhlE proteins is not known.
345 RhlE proteins have been experimentally investigated only in a handful of bacterial species, namely *E.*
346 *coli*, *Y. pseudotuberculosis*, *M. tuberculosis*, *P. syringae* LZ4W (psychotropic strain) and *C. crescentus*
347 (13-19). Importantly, all the bacterial species in which RhlE proteins were studied so far possess one
348 copy of the *rhlE* gene. *P. aeruginosa* genome owns two copies; therefore, it represents an ideal model

349 organism to investigate gene evolution following duplication, assessing conserved and new gene
350 functions. Our phenotypic analysis of *rhlE1* and *rhlE2* mutants confirmed a widespread role of RhlE
351 proteins in sustaining cell growth at cold temperatures, as both *P. aeruginosa rhlE1* and *rhlE2* mutants
352 display a growth defect at 16°C and a growth profile similar to the wild type at 37°C. Cold adaptation
353 is one of the most frequent biological functions associated with RNA helicases. The function is linked
354 to ability of RNA helicases to resolve RNA secondary structures, which are stabilized at low
355 temperatures, allowing the expression of gene(s) essential for growth on cold (15).
356 In addition to cold adaptation, deletion of *rhlE2* in *P. aeruginosa* affects cell motility, reduces biofilm
357 formation and production of virulence factors, ultimately resulting into a significant decrease of lethality
358 in *G. mellonella* infection model. Few other groups of DEAD-box RNA helicases, namely CshA of
359 *Listeria monocytogenes* and *Staphylococcus aureus* and RhpA of *Helicobacter pylori* have been shown
360 to regulate expression of virulence traits (52-54). In addition, another *P. aeruginosa* RNA helicase
361 (PA2840, named DeaD) has been proposed as virulence regulator, due to its stimulatory effect on the
362 synthesis of the type III secretion system regulator ExsA (30). Nonetheless, such an important action
363 as the one of RhlE2 on in vivo host-pathogen interaction is rarely described for a DEAD-box RNA
364 helicase and it has never been observed before for RhlE proteins. Phylogenetic analysis of RhlE proteins
365 indicate that RhlE2 homologs are present in other bacteria phylogenetic distant from *P. aeruginosa*,
366 including environmental bacteria like *Azotobacter vinelandii* and several other bacterial pathogens like
367 *Klebsiella pneumoniae*, *Acinetobacter baumannii*, *Enterobacter clocae* and *Streptococcus dysgalactiae*
368 subsp. *equisimilis* (**Fig S1**), suggesting gene acquisition by horizontal gene transfer. It would be
369 interesting to know whether RhlE2 also plays a role on virulence in other pathogenic species.
370 Contrary to *rhlE2*, *rhlE1* mutation doesn't produce a pleiotropic effect and, when expressed *in trans*,
371 the RhlE1 protein is unable to complement the *rhlE2* mutant phenotypes, indicating that the two proteins
372 act on different targets. In vitro, RhlE1 and RhlE2 possess an ATPase activity strictly RNA-dependent.
373 No base specificity has been observed in our ATPase assays (see 41-mer ssRNA vs U41), but this is
374 not surprising since the RNA helicase catalytic core usually interacts with the 2' OH ribose or the
375 phosphate of the RNA backbone (55). Instead, different RNA preferences are observed depending on

376 RNA length and structure: RhlE1 ATPase is activated by shorter RNA than RhlE2. However, RhlE1 is
377 not sensitive to the RNA structure whereas RhlE2 prefers RNA with a hairpin than RhlE2 (**Fig. 6E**).
378 The difference in RNA length stimulation can be explained by a larger RNA-binding site than on RhlE1
379 or a cooperative binding to RNA. The structure specificity may reflect a hairpin recognition domain on
380 the C-terminal extension. An in-depth biochemical characterization is needed to explore how RhlE2
381 can discriminate RNA secondary structure.
382 At the molecular level, the *P. aeruginosa rhlE2* deleted strain present changes in 15% of the entire
383 cellular transcripts in swarming conditions (N=836 transcripts). Identifying direct targets and assessing
384 interconnection with other regulatory pathways will be the subject of further inquiry. Surprisingly, no
385 discernible changes were observed in the mRNA levels of flagellar and rhamnolipids biosynthesis
386 genes, suggesting that the observed swarming defect of the *rhlE2* mutant might result from a metabolic
387 or energetic imbalance. Another possibility is that the reduced swarming motility of the strain might be
388 linked to the strong down-regulation of the virulence factors elastase LasB and PvdQ, which production
389 is interestingly required for swarming motility (33).
390 In our work, we also show that the RNase E endonuclease, key degradosome component, is co-eluted
391 with FLAG-tagged RhlE2, but not with RhlE1. While studying the giant phage ϕKZ gp37/Dip protein,
392 which interacts with RNase E, Van den Bossche and colleagues recently identified RhlE2 as a possible
393 component of the *P. aeruginosa* degradosome, but the protein was called DeaD as for DEAD-box
394 protein (56). Interaction of RhlE proteins with RNase E is conserved across several bacterial species as
395 it has also been observed previously in *E. coli*, *C. crescentus*, *P. syringae* LZ4W and *M. tuberculosis*
396 (13,17,18,20). In *E. coli*, the RhlE interaction with RNAse E has been observed only in vitro, where the
397 protein can replace the RNA helicases RhlB in facilitating the degradation of structured RNA by
398 PNPase (20). *E. coli* RhlB remains the only helicase with clear role in RNA degradation in vivo and the
399 physiological conditions in which RhlE can replace RhlB are still unknown (57). A RhlB homolog is
400 also present in *P. aeruginosa*, but deletion of the encoding gene doesn't lead to the same phenotypes
401 observed for *rhlE2* mutant (data not shown). Surprisingly, pre-treatment of *P. aeruginosa* cell extracts
402 with RNase A before pull-down affects RhlE2 interaction with RNase E. The same experiment was

403 performed in *C. crescentus*, but in that case the interaction resisted to the treatment (13). These results
404 indicate that, while in *C. crescentus* interaction of RhlE with RNase E is a protein-protein interaction,
405 *P. aeruginosa* interaction of RhlE2 with RNase E is mediated or stabilized by RNA. The C-terminal
406 extension of RhlE2 is necessary for the observed interaction, as RNase E does not interact with $RhlE2_{1-}$
407 $_{434}$ construct in bacterial two-hybrid assays (**Fig S8**). The $RhlE2_{1-434}$ protein shows in vitro an RNA-
408 dependent ATPase activity similar to the full-length protein, but it does not restore in vivo the *rhlE2*
409 mutant phenotypes to wild type levels, suggesting that RhlE2 performs its regulatory action via the
410 RNA degradosome. Indeed, we show that RhlE2 affects the half-life of some of the transcripts whose
411 levels were affected by *rhlE2* deletion in the RNA-sequencing analysis. In *E. coli*, RNase E was shown
412 to interact with RhlB by binding to the RecA2 domain and stimulating its ATPase activity (58,59). We
413 do not observe stimulation of RhlE2 activity by RNase E (data not shown), probably due to the different
414 type of interactions these two helicases enact with the endonuclease. Our work on RhlE2 hints that *P.*
415 *aeruginosa* RNA degradosome mode of action might differ from *E. coli*, as also suggested when looking
416 at RNase E sequence conservation among these two species (60). We are currently investigating this
417 matter.
418

419 **Acknowledgements**

420 We are grateful to Patrick Linder for critical reading of the manuscript. RNA-sequencing experiments
421 were performed at the iGE3 genomics platform of the University of Geneva while MS/MS protein
422 identifications were performed at the proteomics core facility of the Faculty of Medicine (University of
423 Geneva), and we are very grateful for their help and advices.
424

425 **Funding**

426 This work was supported by a Swiss National Science Foundation Ambizione grant (PZ00P3_174063
427 to M.V.), the Novartis Foundation for medical-biological Research and The Sir Jules Thorn Charitable
428 Overseas Trust (M.V.).

429 **Materials and Methods**

430 **Bacterial strains and culture conditions.** Bacterial strains and plasmids used in this study are listed
431 in **Table S4**. Cells were grown in Luria Broth (LB) or nutrient yeast broth (NYB) (61,62) medium, with
432 shaking at 180 rpm and at 37°C. Nutrient agar (NA) was used as a solid medium. When required,
433 antibiotics were added to these media at the following concentrations: 100 µg/ml ampicillin, 25 µg/ml
434 tetracycline and 10 µg/ml gentamicin for *E. coli*; and 50 µg/ml gentamicin and 50 µg/ml tetracycline
435 for *P. aeruginosa*.

436 **Genetic techniques.** DNA cloning and plasmid preparation were performed according to standard
437 methods (63). Oligonucleotides used for cloning procedures are listed in **Table S5**. Restriction and
438 DNA-modifying enzymes were used following the instructions of the manufacturers. Transformation
439 of *E. coli* DH5α, *E. coli* TOP10 (for cloning) and *P. aeruginosa* was carried out by heat-shock and
440 electroporation, respectively (64). The construction of engineered plasmids and strains is detailed in
441 Supplemental Material. All plasmids and strains were verified by PCR and sequencing.

442 **RhlE1 and RhlE2 purifications**. The pET28-His_{10}Smt3-RhlE1 and RhlE2 plasmids were transformed
443 into *E. coli* BL21(DE3). Cultures (500 ml) derived from single transformants were grown at 37°C in
444 LB medium containing 50 µg/ml kanamycin until the OD_{600} reached 0.6. The cultures were adjusted to
445 0.2 mM IPTG and 2% (v/v) ethanol and incubation was continued for 20 h at 17˚C. Cells were harvested
446 by centrifugation and stored at -80˚C. All subsequent procedures were performed at 4˚C. Thawed
447 bacteria were resuspended in 25 ml of buffer A (50 mM Tris-HCl, pH 8.0, 500 mM NaCl, 10% glycerol)
448 and supplemented with one tablet of protease inhibitor cocktail (Roche). The suspension was adjusted
449 to 0.1 mg/ml lysozyme and incubated on ice for 30 min. Imidazole and Triton-X100 were added to a
450 final concentration of 10 mM and 0.1%, respectively. The lysate was sonicated to reduce viscosity and
451 insoluble material was removed by centrifugation. The soluble extracts were applied to a 1 ml of Ni^{2+}-
452 NTA-agarose (Qiagen) column that had been equilibrated with buffer A containing 10 mM imidazole.
453 The column was washed with 10 ml aliquots of 20 mM imidazole in buffer A and then eluted stepwise
454 with 3 ml aliquots of buffer A containing 50, 100, 250, and 500 mM imidazole, respectively. The elution
455 profiles were monitored by SDS-PAGE (not shown; 250 mM imidazole fraction is shown in Fig 5A).

456 The recombinant His10Smt3-RhlE polypeptides were recovered predominantly in the 250 mM
457 imidazole fractions. The protein concentration of the 250 mM imidazole eluate fraction was determined
458 using the Bio-Rad dye reagent with BSA as the standard. Proteins concentration were calculated by
459 interpolation to the BSA standard curve. RhlE1 and RhlE2 mutated variants were produced and purified
460 as described above for the wild type RhlE1 and RhlE2.

461 **ATPase reaction**. Reaction mixtures (15 µl) containing 50 mM Tris-HCl, pH 8.0, 5 mM DTT, 2m
462 MgCl2, 1mM ATP, RNA as specified, and enzyme as specified were incubated for 15 min at 37°C. The
463 reactions were quenched by adding 3.8 µl of 5 M formic acid. Aliquots (2 µl) were applied to a
464 polyethylenimine(PEI)-cellulose thin layer chromatography (TLC) plates (Merk), which were
465 developed with 1 M formic acid, 0.5 M LiCl. ^{32}Pi release was quantitated by scanning the chromatogram
466 with laser Scanner Typhoon FLA 7000 (General Electric).

467 **β-Galactosidase assays.** β-Galactosidase experiments were performed as described previously (62),
468 with *P. aeruginosa* strains grown in NYB medium. Data are mean values of three independent samples
469 ± standard deviations.

470 **Phenotypic assays.** *Growth assays.* Liquid growth assays at 25, 37 and 43°C were performed in 96-
471 well plates each containing 200 µl of LB and cell density (OD 600) was measured with a Synergy H1
472 plate reader (Biotek). Spot assays were performed by spotting 10 µl of serial dilutions of cultures (at
473 initial OD600 of 1.0) on LB plates incubated at 16 °C or at 37 °C. *Biofilm formation.* Quantification of
474 biofilm formation was performed in 24-well polystyrene microtiter plates as previously described (65).
475 The plates were incubated for 10 h at 37°C and biofilms were stained with 0.1% crystal violet solution.
476 The dye bound, which is proportional to the biofilm produced, was solubilized with 96% (v/v) ethanol
477 and the absorption was photometrically measured at 600 nm (OD_{600}). Data are mean values of three
478 independent samples ± standard deviations. *Motility assays.* Motility assays were carried out essentially
479 as previously described (66,67). Swim assays were carried out on 10 g/L tryptone, 5 g/L NaCl, 0.3%
480 agar (Merck) plates. 0.5 µl of standardized overnight culture was injected below the surface of the agar
481 and plates were incubated at 30°C overnight. Twitch assays were carried out on 1% LB agar plates and
482 bacteria were inoculated by picking a colony using a sterile tip and stabbing to the bottom of the plates,

483 which were incubated at 37°C for two days. The agar was then peeled off the plate, and cells were
484 stained with crystal violet for visualization. Swarming assays were performed in plates consisted of
485 0.5% (wt/vol) Difco bacto-agar with either 8 g/liter Difco nutrient broth and 5 g/liter glucose or with
486 MMP MMP medium supplemented with 20 mM glucose and 0.1% (w/v) casamino acids (66,68). Cells
487 were inoculated onto swarm plates using 5µl of standardized overnight cultures and incubated overnight
488 at 37°C. Pictures are taken from a representative plate out of five independent experiments. Swarming
489 complementation experiments were performed in 0.5% (wt/vol) nutrient agar plus 0.2% arabinose.
490 Pictures are taken from a representative motility plate out of five independent experiments. ImageJ
491 software (NIH) was used to determine the area of the plate surface covered by the bacteria as previously
492 described (69).

493 **Bacterial two-hybrid assay.** Bacterial two hybrid experiments (70). Recombinant pKT25 and pUT18C
494 derivative plasmids were transformed simultaneously into the *E. coli* BTH101 strain. Transformants
495 were spotted onto McConkey agar plates supplemented with 1mM isopropyl β-d-thiogalactoside
496 (IPTG) in the presence of 100 µg/ml ampicillin, 50 µg/ml kanamycin, and 100 µg/ml 5-bromo-4-chloro-
497 indolyl-β-d-galactopyranoside (X-gal). Positive interactions were identified as blue colonies after 24h
498 incubation at 30°C and quantified by β-galactosidase assays. The positive controls used in the study
499 were pUT18C and pKT25 derivatives encoding the leucine zipper from GCN4 (zip), which strongly
500 dimerizes. Data are mean values of three independent samples ± standard deviations.

501 **Virulence factor production assays.** *Elastase production.* The LasB elastase activity of bacterial
502 suspensions was determined with the Elastin-Congo red (ECR; Sigma, St. Louis, MO) assay, as
503 previously described (71). Briefly, 50 µl aliquots of filtered bacterial supernatant of a 21 h culture were
504 added to 900 µl of ECR buffer (100 mM Tris, 1 mM CaCl2, pH 7.5) containing 20 mg of ECR and then
505 incubated with shaking at 37°C for 18 h. Insoluble ECR was removed by centrifugation and the
506 absorption of the supernatant was measured at 495 nm and normalized according to cell density
507 (OD600). LB medium was used as a negative control. *Pyocyanin production.* Pyocyanin quantification
508 was performed using the assay based on absorbance at 520 nm in an acidic solution. Briefly, 5 ml
509 supernatant from a stationary phase culture was mixed with 3 ml of chloroform. Pyocyanin from the

510 organic phase was then extracted with 1 ml of 0.2 N HCl, and absorbance was measured at 520 nm.
511 Concentrations, expressed as micrograms of pyocyanin produced per milliliter of culture supernatant,
512 were determined by multiplying the optical density at 520 nm by 17.072 (72). The experiment was
513 conducted three times in independent experiments.

514 **In vivo virulence assays**. The wax moth model *Galleria mellonella* was used for *in vivo* virulence
515 assays, as previously described (73). Briefly, overnight cultures were diluted 1:100 and sub-cultured (3
516 ml LB) at 37°C until exponential phase (3 hours). Bacterial cells (OD600 = 1.0) were washed with PBS
517 three times. The samples were serially diluted (up to 10−7) and a 10 µl volume of the dilutions was
518 spotted on LB agar and CFU counted the next day. A 10 µl volume of the 10−7 dilution for the wild
519 type and mutant strains was injected into the last abdominal proleg of ten larvae per sample. An
520 additional ten larvae were injected with PBS as negative control. Larvae mortality was monitored every
521 two hours from 16 to 40 hrs post-infection (larvae are considered dead when they turn black and do not
522 respond to tapping). All data are mean values of three independent samples ± standard deviation.

523 **Total RNA extraction.** PAO1 wild type, PAO1Δ*rhlE1*, PAO1Δ*rhlE2* and PAO1Δ*rhlE1*Δ*rhlE2*
524 mutants were grown at 37°C in swarming condition or on NYB until OD~1.5 with vigorous shaking.
525 Cells were harvested using the RNA bacteria protect solution (QIAGEN). Total RNAs was extracted
526 and purified using Monarch RNA isolation kit (NEB), treated with DNase I (Promega) three times to
527 remove contaminating genomic DNA and re-purified again using phenol-chloroform. Eventual DNA
528 contamination was tested by PCR with 40 cycles and different couples of primers (**Table S5**) and RNA
529 integrity was controlled by agarose gel electrophoresis.

530 **RNA sequencing.** PAO1 wild type, PAO1Δ*rhlE1*, PAO1Δ*rhlE2* and PAO1Δ*rhlE1*Δ*rhlE2* mutants
531 were grown in twelve 12-cm square swarming plates. After O/N incubation at 37°C, samples from 6
532 plates were pooled and total RNA was isolated from as described above. Two replicates of either strain
533 were therefore obtained. Ribosomal RNA was depleted with Ribo-Zero rRNA Removal Kit (Illumina).
534 Then, libraries were prepared using the Illumina TruSeq stranded mRNA kit and validated on the
535 Bioanalyzer 2100 (Agilent). Samples were sequenced using the Illumina HiSeq 2000, 100 bp single end
536 read at the iGE3 genomics platform of the University of Geneva. After removal of the adaptors, the

537 sequences were quality trimmed with trimmomatic using default parameters (74). The resulting
538 sequences were then mapped onto the PAO1 reference genome (NC_002516.2) using Segemehl (74).
539 For differential gene expression analysis, reads were counted using the DESeq2 package (75). All RNAs
540 with a log2-fold change greater than 2 and a multiple testing adjusted p-value below 0.05 were
541 considered differentially abundant.

542 **Real-time quantitative PCR (RT-qPCR).** cDNAs from RNA isolated sample was obtained using M-
543 MLV reverse transcriptase (Promega) following the manufacturer instructions. Resultant cDNAs were
544 used as template for qPCR and qPCR was performed on an Applied Biosystems 7900HT Sequence
545 Detection system using a Sybr Green Quantitect kit (QIAGEN, Hildesheim, Germany). Quantification
546 cycle (Cq; standard name for Ct or Cp value) values were recorded with SDS version 2.3 software. Cq
547 values ≥36 were considered beyond the limit of detection. Fold changes were determined using the
548 relative quantification comparative threshold cycle (C_t) method ($\Delta\Delta C_t$) and normalization was done by
549 comparison with *rplA*, *oprD* and *rpoD* housekeeping genes as reference genes. The primer pairs that
550 were used for qRT-PCR are shown in **Table S3**. For each gene tested, a standard curve was made using
551 serial dilutions from 50 to 0.005 ng of *P. aeruginosa* PAO1 genomic DNA in order to quantify the
552 efficiency of every PCR reaction. The PCR products were ranging between 150 and 200 bp in length.
553 All data are mean values of three independent samples and three technical replicates.

554 **RNA decay analysis**. For decay analysis, rifampicin to 250 µg/ml was added to PAO1 wild type,
555 PAO1Δ*rhlE2* liquid culture grown to OD600 of ~1.5 and aliquots were withdrawn at the indicated
556 times. RNA was extracted and used for RT-qPCR analysis using primers listed in **Table S3.**

557 **Pull-down assays.** PAO1Δ*rhlE1*::P_{BAD}-3xFLAG_RhlE1, PAO1Δ*rhlE2*::P_{BAD}_RhlE2,
558 PAO1Δ*rhlE2*::P_{BAD}-3xFLAG_RhlE2 and PAO1Δ*rhlE2*::P_{BAD}-3xFLAG_RhlE2$_{1-434}$ cultures were
559 grown in 2L flasks with 400 ml NYB plus 0.05% arabinose to an O.D ~1.8-2.0, then pelleted by
560 centrifugation and stored at -80°C for at least 12 hours. Pellets were re-suspended in ice-cold IP buffer
561 (20 mM HEPES pH 7.4, 300 mM NaCl, 1 mM EDTA, protease inhibitor) and cells were lysed by
562 sonication. Samples were then centrifuged (15,000 g, 60 min, 4°C), the supernatant (soluble fraction)
563 was collected and 1.0% v/v Triton X-100 was added and incubated at 4°C with end-over-end agitation

564 for 20 minutes. Then, samples were incubated for 4 hours with 20 µg/ml ANTI-FLAG M2 affinity gel
565 (Sigma) (4°C, end-over-end agitation). Samples were pelleted by centrifugation (3,000 g, 1 min 4°C),
566 the supernatant was discarded, and the beads re-suspended in 1.0 ml ice-cold IP buffer. This wash step
567 was repeated 5 times. Elution was performed twice in 100 µl 3xFLAG peptide (Sigma) at final
568 concentration of 100 µg/ml. The presence of Flag-tagged RhlE proteins was confirmed by
569 immunoblotting, and co-eluting proteins were detected by Orbitrap mass spectrometry or by SDS-page
570 followed by protein band extraction and identification by mass spectrometry.
571 **Phylogenetic analysis.** Sequences were retrieved from the NCBI RefSeq database (76) and aligned
572 with MUSCLE (77). Sequences of RecQ (PA3344) were added as outgroup.
573

References

1. Valentini, M. and Linder, P. (2021) Happy Birthday: 30 Years of RNA Helicases. *Methods in molecular biology (Clifton, N.J.)*, **2209**, 17-34.
2. Linder, P., Lasko, P.F., Ashburner, M., Leroy, P., Nielsen, P.J., Nishi, K., Schnier, J. and Slonimski, P.P. (1989) Birth of the D-E-A-D box. *Nature*, **337**, 121-122.
3. Gorbalenya, A.E. and Koonin, E.V. (1993) Helicases: amino acid sequence comparisons and structure-function relationships. *Current Opinion in Structural Biology*, **3**, 419-429.
4. Linder, P. and Daugeron, M.C. (2000) Are DEAD-box proteins becoming respectable helicases? *Nature structural biology*, **7**, 97-99.
5. Fiorini, F., Boudvillain, M. and Le Hir, H. (2012) Tight intramolecular regulation of the human Upf1 helicase by its N- and C-terminal domains. *Nucleic Acids Res*, **41**, 2404-2415.
6. Pietras, Z., Hardwick, S.W., Swiezewski, S. and Luisi, B.F. (2013) Potential regulatory interactions of Escherichia coli RraA protein with DEAD-box helicases. *The Journal of biological chemistry*, **288**, 31919-31929.
7. Kossen, K., Karginov, F.V. and Uhlenbeck, O.C. (2002) The carboxy-terminal domain of the DExDH protein YxiN is sufficient to confer specificity for 23S rRNA. *Journal of molecular biology*, **324**, 625-636.
8. Diges, C.M. and Uhlenbeck, O.C. (2001) *Escherichia coli* DbpA is an RNA helicase that requires hairpin 92 of 23S rRNA. *The EMBO journal*, **20**, 5503-5512.
9. Redder, P., Hausmann, S., Khemici, V., Yasrebi, H. and Linder, P. (2015) Bacterial versatility requires DEAD-box RNA helicases. *FEMS microbiology reviews*, **39**, 392-412.
10. Kaberdin, V.R. and Bläsi, U. (2013) Bacterial helicases in post-transcriptional control. *Biochimica et biophysica acta*, **1829**, 878-883.
11. Owttrim, G.W. (2013) RNA helicases: diverse roles in prokaryotic response to abiotic stress. *RNA biology*, **10**, 96-110.
12. Lopez-Ramirez, V., Alcaraz, L.D., Moreno-Hagelsieb, G. and Olmedo-Alvarez, G. (2011) Phylogenetic distribution and evolutionary history of bacterial DEAD-Box proteins. *J Mol Evol*, **72**, 413-431.
13. Aguirre, A.A., Vicente, A.M., Hardwick, S.W., Alvelos, D.M., Mazzon, R.R., Luisi, B.F. and Marques, M.V. (2017) Association of the Cold Shock DEAD-Box RNA Helicase RhlE to the RNA Degradosome in *Caulobacter crescentus*. *Journal of bacteriology*, **199**, e00135-00117.
14. Virtanen, J.P., Keto-Timonen, R., Jaakkola, K., Salin, N. and Korkeala, H. (2018) Changes in Transcriptome of *Yersinia pseudotuberculosis* IP32953 Grown at 3 and 28°C Detected by RNA Sequencing Shed Light on Cold Adaptation. *Front Cell Infect Microbiol*, **8**, 2235-2988 (Electronic).
15. Awano, N., Xu, C., Ke, H., Inoue, K., Inouye, M. and Phadtare, S. (2007) Complementation analysis of the cold-sensitive phenotype of the *Escherichia coli csdA* deletion strain. *Journal of bacteriology*, **189**, 5808-5815.
16. Ohmori, H. (1994) Structural analysis of the *rhlE* gene of *Escherichia coli*. *Idengaku zasshi*, **69**, 1-12.
17. Płociński, P., Macios, M., Houghton, J., Niemiec, E., Płocińska, R., Brzostek, A., Słomka, M., Dziadek, J., Young, D. and Dziembowski, A. (2019) Proteomic and transcriptomic experiments reveal an essential role of RNA degradosome complexes in shaping the transcriptome of *Mycobacterium tuberculosis*. *Nucleic acids research*, **47**, 5892-5905.
18. Purusharth, R.I., Klein, F., Sulthana, S., Jäger, S., Jagannadham, M.V., Evguenieva-Hackenberg, E., Ray, M.K. and Klug, G. (2005) Exoribonuclease R interacts with endoribonuclease E and an RNA helicase in the psychrotrophic bacterium *Pseudomonas syringae* Lz4W. *The Journal of biological chemistry*, **280**, 14572-14578.
19. Jain, C. (2008) The *E. coli* RhlE RNA helicase regulates the function of related RNA helicases during ribosome assembly. *RNA (New York, N.Y.)*, **14**, 381-389.

20. Khemici, V., Toesca, I., Poljak, L., Vanzo, N.F. and Carpousis, A.J. (2004) The RNase E of Escherichia coli has at least two binding sites for DEAD-box RNA helicases: functional replacement of RhlB by RhlE. *Molecular microbiology*, **54**, 1422-1430.
21. Green, S.K., Schroth, M.N., Cho, J.J., Kominos, S.K. and Vitanza-jack, V.B. (1974) Agricultural plants and soil as a reservoir for *Pseudomonas aeruginosa*. *Applied microbiology*, **28**, 987-991.
22. Hardalo, C. and Edberg, S.C. (1997) *Pseudomonas aeruginosa*: assessment of risk from drinking water. *Critical reviews in microbiology*, **23**, 47-75.
23. Palleroni, N.J. (2015) Pseudomonas. *Bergey's Manual of Systematics of Archaea and Bacteria*, 1-1.
24. Garcia-Clemente, M., de la Rosa, D., Máiz, L., Girón, R., Blanco, M., Olveira, C., Canton, R. and Martinez-García, M.A. (2020) Impact of Pseudomonas aeruginosa Infection on Patients with Chronic Inflammatory Airway Diseases. *Journal of clinical medicine*, **9**.
25. Urwin, L., Okurowska, K., Crowther, G., Roy, S., Garg, P., Karunakaran, E., MacNeil, S., Partridge, L.J., Green, L.R. and Monk, P.N. (2020) Corneal Infection Models: Tools to Investigate the Role of Biofilms in Bacterial Keratitis. *Cells*, **9**.
26. Costerton, J.W., Stewart, P.S. and Greenberg, E.P. (1999) Bacterial biofilms: a common cause of persistent infections. *Science (New York, N.Y.)*, **284**, 1318-1322.
27. De Oliveira, D.M.P., Forde, B.M., Kidd, T.J., Harris, P.N.A., Schembri, M.A., Beatson, S.A., Paterson, D.L. and Walker, M.J. (2020) Antimicrobial Resistance in ESKAPE Pathogens. *Clinical microbiology reviews*, **33**.
28. Pendleton, J.N., Gorman, S.P. and Gilmore, B.F. (2013) Clinical relevance of the ESKAPE pathogens. *Expert review of anti-infective therapy*, **11**, 297-308.
29. Lyczak, J.B., Cannon, C.L. and Pier, G.B. (2000) Establishment of *Pseudomonas aeruginosa* infection: lessons from a versatile opportunist. *Microbes and infection*, **2**, 1051-1060.
30. Intile, P.J., Balzer, G.J., Wolfgang, M.C. and Yahr, T.L. (2015) The RNA helicase DeaD stimulates ExsA translation to promote expression of the *Pseudomonas aeruginosa* type III secretion system. *Journal of bacteriology*, **197**, 2664-2674.
31. Kearns, D.B. (2010) A field guide to bacterial swarming motility. *Nature reviews. Microbiology*, **8**, 634-644.
32. Tremblay, J. and Déziel, E. (2010) Gene expression in *Pseudomonas aeruginosa* swarming motility. *BMC Genomics*, **11**, 587.
33. Overhage, J., Bains M Fau - Brazas, M.D., Brazas Md Fau - Hancock, R.E.W. and Hancock, R.E. (2008) Swarming of *Pseudomonas aeruginosa* is a complex adaptation leading to increased production of virulence factors and antibiotic resistance. *Journal of bacteriology*, **190**, 2671-2679.
34. Merritt, J.H., Ha, D.G., Cowles, K.N., Lu, W., Morales, D.K., Rabinowitz, J., Gitai, Z. and O'Toole, G.A. (2010) Specific control of *Pseudomonas aeruginosa* surface-associated behaviors by two c-di-GMP diguanylate cyclases. *mBio*, **1**.
35. Watanabe, S., Morimoto, D., Fukumori, F., Shinomiya, H., Nishiwaki, H., Kawano-Kawada, M., Sasai, Y., Tozawa, Y. and Watanabe, Y. (2012) Identification and characterization of D-hydroxyproline dehydrogenase and Delta1-pyrroline-4-hydroxy-2-carboxylate deaminase involved in novel L-hydroxyproline metabolism of bacteria: metabolic convergent evolution. *The Journal of biological chemistry*, **287**, 32674-32688.
36. McIver, K.S., Kessler, E., Olson, J.C. and Ohman, D.E. (1995) The elastase propeptide functions as an intramolecular chaperone required for elastase activity and secretion in *Pseudomonas aeruginosa*. *Molecular microbiology*, **18**, 877-889.
37. McMorran, B.J., Kumara, H., Sullivan, K. and Lamont, I.L. (2001) Involvement of a transformylase enzyme in siderophore synthesis in *Pseudomonas aeruginosa*. *Microbiology (Reading, England)*, **147**, 1517-1524.
38. Déziel, E., Lépine, F., Milot, S. and Villemur, R. (2003) *rhlA* is required for the production of a novel biosurfactant promoting swarming motility in *Pseudomonas aeruginosa*: 3-(3-hydroxyalkanoyloxy)alkanoic acids (HAAs), the precursors of rhamnolipids. *Microbiology (Reading, England)*, **149**, 2005-2013.

39. Passador, L., Cook, J.M., Gambello, M.J., Rust, L. and Iglewski, B.H. (1993) Expression of *Pseudomonas aeruginosa* virulence genes requires cell-to-cell communication. *Science (New York, N.Y.)*, **260**, 1127-1130.
40. Brint, J.M. and Ohman, D.E. (1995) Synthesis of multiple exoproducts in *Pseudomonas aeruginosa* is under the control of RhlR-RhlI, another set of regulators in strain PAO1 with homology to the autoinducer-responsive LuxR-LuxI family. *Journal of bacteriology*, **177**, 7155-7163.
41. Lau, G.W., Hassett, D.J., Ran, H. and Kong, F. (2004) The role of pyocyanin in *Pseudomonas aeruginosa* infection. *Trends in molecular medicine*, **10**, 599-606.
42. Junqueira, J.C. (2012) Galleria mellonella as a model host for human pathogens. *Virulence*, **3**, 474-476.
43. Putnam, A.A. and Jankowsky, E. (2013) DEAD-box helicases as integrators of RNA, nucleotide and protein binding. *Biochimica et biophysica acta*, **1829**, 884-893.
44. Tauchert, M.J., Fourmann, J.B., Luhrmann, R. and Ficner, R. (2017) Structural insights into the mechanism of the DEAH-box RNA helicase Prp43. *eLife*, **6**.
45. Boneberg, F.M., Brandmann, T., Kobel, L., van den Heuvel, J., Bargsten, K., Bammert, L., Kutay, U. and Jinek, M. (2019) Molecular mechanism of the RNA helicase DHX37 and its activation by UTP14A in ribosome biogenesis. *RNA (New York, N.Y.)*, **25**, 685-701.
46. Prabu, J.R., Muller, M., Thomae, A.W., Schussler, S., Bonneau, F., Becker, P.B. and Conti, E. (2015) Structure of the RNA Helicase MLE Reveals the Molecular Mechanisms for Uridine Specificity and RNA-ATP Coupling. *Molecular cell*, **60**, 487-499.
47. Karimova, G., Pidoux, J., Ullmann, A. and Ladant, D. (1998) A bacterial two-hybrid system based on a reconstituted signal transduction pathway. *Proceedings of the National Academy of Sciences*, **95**, 5752.
48. Xu, L., Wang, L., Peng, J., Li, F., Wu, L., Zhang, B., Lv, M., Zhang, J., Gong, Q., Zhang, R. *et al.* (2017) Insights into the Structure of Dimeric RNA Helicase CsdA and Indispensable Role of Its C-Terminal Regions. *Structure (London, England : 1993)*, **25**, 1795-1808.e1795.
49. Giraud, C., Hausmann, S., Lemeille, S., Prados, J., Redder, P. and Linder, P. (2015) The C-terminal region of the RNA helicase CshA is required for the interaction with the degradosome and turnover of bulk RNA in the opportunistic pathogen Staphylococcus aureus. *RNA biology*, **12**, 658-674.
50. Apirion, D. (1978) Isolation, genetic mapping and some characterization of a mutation in *Escherichia coli* that affects the processing of ribonuleic acid. *Genetics*, **90**, 659-671.
51. Vasil, M.L. (1986) *Pseudomonas aeruginosa*: biology, mechanisms of virulence, epidemiology. *The Journal of pediatrics*, **108**, 800-805.
52. El Mortaji, L., Aubert, S., Galtier, E., Schmitt, C., Anger, K., Redko, Y., Quentin, Y. and De Reuse, H. (2018) The Sole DEAD-Box RNA Helicase of the Gastric Pathogen *Helicobacter pylori* Is Essential for Colonization. *mBio*, **9**, e02071-02017.
53. Netterling, S., Bäreclev, C., Vaitkevicius, K. and Johansson, J. (2016) RNA Helicase Important for *Listeria monocytogenes* Hemolytic Activity and Virulence Factor Expression. *Infection and Immunity*, **84**, 67.
54. Oun, S., Redder, P., Didier, J.P., François, P., Corvaglia, A.R., Buttazzoni, E., Giraud, C., Girard, M., Schrenzel, J. and Linder, P. (2013) The CshA DEAD-box RNA helicase is important for quorum sensing control in *Staphylococcus aureus*. *RNA biology*, **10**, 157-165.
55. Ozgur, S., Buchwald, G., Falk, S., Chakrabarti, S., Prabu, J.R. and Conti, E. (2015) The conformational plasticity of eukaryotic RNA-dependent ATPases. *The FEBS journal*, **282**, 850-863.
56. Van den Bossche, A., Hardwick, S.W., Ceyssens, P.J., Hendrix, H., Voet, M., Dendooven, T., Bandyra, K.J., De Maeyer, M., Aertsen, A., Noben, J.P. *et al.* (2016) Structural elucidation of a novel mechanism for the bacteriophage-based inhibition of the RNA degradosome. *eLife*, **5**.
57. Khemici, V., Poljak, L., Toesca, I. and Carpousis, A.J. (2005) Evidence in vivo that the DEAD-box RNA helicase RhlB facilitates the degradation of ribosome-free mRNA by RNase E. *Proc Natl Acad Sci U S A*, **102**, 6913-6918.

731 58. Chandran, V., Poljak, L., Vanzo, N.F., Leroy, A., Miguel, R.N., Fernandez-Recio, J.,
732 Parkinson, J., Burns, C., Carpousis, A.J. and Luisi, B.F. (2007) Recognition and cooperation
733 between the ATP-dependent RNA helicase RhlB and ribonuclease RNase E. *Journal of*
734 *molecular biology*, **367**, 113-132.
735 59. Bruce, H.A., Du, D., Matak-Vinkovic, D., Bandyra, K.J., Broadhurst, R.W., Martin, E., Sobott,
736 F., Shkumatov, A.V. and Luisi, B.F. (2018) Analysis of the natively unstructured RNA/protein-
737 recognition core in the *Escherichia coli* RNA degradosome and its interactions with regulatory
738 RNA/Hfq complexes. *Nucleic acids research*, **46**, 387-402.
739 60. Aït-Bara, S., Carpousis, A.J. and Quentin, Y. (2015) RNase E in the γ-Proteobacteria:
740 conservation of intrinsically disordered noncatalytic region and molecular evolution of
741 microdomains. *Molecular Genetics and Genomics*, **290**, 847-862.
742 61. Sezonov, G., Joseleau-Petit, D. and D'Ari, R. (2007) Escherichia coli physiology in Luria-
743 Bertani broth. *J Bacteriol*, **189**, 8746-8749.
744 62. Miller, J.H. (1972) *Experiments in molecular genetics*, Cold Spring Harbor Laboratory, Cold
745 Spring Harbor, NY.
746 63. Sambrook, J., E. F. Fritsch, and T. Maniatis. (1989) *Molecular cloning: a laboratory manual*.
747 2nd ed. ed, 2nd ed. Cold Spring Harbor Laboratory Press. Cold Spring Harbor, NY.
748 64. Pessi, G. and Haas, D. (2000) Transcriptional control of the hydrogen cyanide biosynthetic
749 genes hcnABC by the anaerobic regulator ANR and the quorum-sensing regulators LasR and
750 RhlR in *Pseudomonas aeruginosa*. *J Bacteriol*, **182**, 6940-6949.
751 65. Moscoso, J.A., Jaeger, T., Valentini, M., Hui, K., Jenal, U. and Filloux, A. (2014) The
752 diguanylate cyclase SadC is a central player of the Gac/Rsm-mediated biofilm formation in
753 Pseudomonas aeruginosa. *Journal of bacteriology*.
754 66. Rashid, M.H. and Kornberg, A. (2000) Inorganic polyphosphate is needed for swimming,
755 swarming, and twitching motilities of Pseudomonas aeruginosa. *Proceedings of the National*
756 *Academy of Sciences of the United States of America*, **97**, 4885-4890.
757 67. Mikkelsen, H., Ball, G., Giraud, C. and Filloux, A. (2009) Expression of Pseudomonas
758 aeruginosa CupD fimbrial genes is antagonistically controlled by RcsB and the EAL-containing
759 PvrR response regulators. *PloS one*, **4**, e6018.
760 68. Wenner, N., Maes, A., Cotado-Sampayo, M. and Lapouge, K. (2014) NrsZ: a novel, processed,
761 nitrogen-dependent, small non-coding RNA that regulates Pseudomonas aeruginosa PAO1
762 virulence. *Environmental microbiology*, **16**, 1053-1068.
763 69. Valentini, M., Laventie, B.J., Moscoso, J., Jenal, U. and Filloux, A. (2016) The Diguanylate
764 Cyclase HsbD Intersects with the HptB Regulatory Cascade to Control Pseudomonas
765 aeruginosa Biofilm and Motility. *PLoS genetics*, **12**, e1006354.
766 70. Bordi, C., Lamy, M.C., Ventre, I., Termine, E., Hachani, A., Fillet, S., Roche, B., Bleves, S.,
767 Mejean, V., Lazdunski, A. *et al.* (2010) Regulatory RNAs and the HptB/RetS signalling
768 pathways fine-tune Pseudomonas aeruginosa pathogenesis. *Molecular microbiology*, **76**, 1427-
769 1443.
770 71. Dieppois, G., Ducret, V., Caille, O. and Perron, K. (2012) The transcriptional regulator CzcR
771 modulates antibiotic resistance and quorum sensing in *Pseudomonas aeruginosa*. *PloS one*, **7**,
772 e38148.
773 72. Essar, D.W., Eberly, L., Hadero, A. and Crawford, I.P. (1990) Identification and
774 characterization of genes for a second anthranilate synthase in *Pseudomonas aeruginosa*:
775 interchangeability of the two anthranilate synthases and evolutionary implications. *Journal of*
776 *bacteriology*, **172**, 884-900.
777 73. McCarthy, R.R., Valentini, M. and Filloux, A. (2017) Contribution of Cyclic di-GMP in the
778 Control of Type III and Type VI Secretion in Pseudomonas aeruginosa. *Methods in molecular*
779 *biology (Clifton, N.J.)*, **1657**, 213-224.
780 74. Bolger, A.M., Lohse, M. and Usadel, B. (2014) Trimmomatic: a flexible trimmer for Illumina
781 sequence data. *Bioinformatics*, **30**, 2114-2120.
782 75. Love, M.I., Huber, W. and Anders, S. (2014) Moderated estimation of fold change and
783 dispersion for RNA-seq data with DESeq2. *Genome Biology*, **15**, 550.

76. Pruitt, K.D., Brown, G.R., Hiatt, S.M., Thibaud-Nissen, F., Astashyn, A., Ermolaeva, O., Farrell, C.M., Hart, J., Landrum, M.J., McGarvey, K.M. *et al.* (2014) RefSeq: an update on mammalian reference sequences. *Nucleic acids research*, **42**, D756-763.
77. Edgar, R.C. (2004) MUSCLE: multiple sequence alignment with high accuracy and high throughput. *Nucleic acids research*, **32**, 1792-1797.

791 **FIGURES LEGENDS**

792

793 **Figure 1. Phylogenetic tree of the bacterial RhlE DEAD-box proteins. (A)** The tree is based on 799
794 sequences of bacterial DEAD-box proteins, found in the NCBI RefSeq database. The *P. aeruginosa*
795 RecQ protein (PA3344) has been used to root the tree. At least 8 distinct lineages can readily be
796 identified and are divided into group I to VIII. **(B)** Linear representation of *P. aeruginosa* (Pa) RhlE1
797 (E1, PA3950) and RhlE2 (E2, PA0428) with the RecA1 and RecA2 domains in white boxes and their
798 C-terminal extension (CTE) in green and blue boxes, respectively. % indicates sequence identity with
799 *E. coli* RhlE protein. Lines corresponds to recombinantly produced RhlE1 and RhlE2 variants (K51A
800 and 1-434)

801

802 **Figure 2. Role of RhlE1 and RhlE2 in *P. aeruginosa* cold adaptation. (A)** 37 °C and **(B)** cold shock
803 (16 °C) survival assays of wild type PAO1, Δ*rhlE1* mutant (ΔE1), Δ*rhlE2* mutant (ΔE2) and
804 Δ*rhlE1*Δ*rhlE2* mutant (ΔE1ΔE2). **(C)** Complementation effects of cold (16 °C) growth using mini-Tn7
805 constructs expressing 3xFLAG-tagged RhlE1 (::3xFLAG-E1), 3xFLAG-tagged RhlE2 (::3xFLAG-
806 E2), **(D)**, 3xFLAG-tagged $RhlE1_{K51A}$ (::3xFLAG-$E1_{K51A}$), 3xFLAG-tagged $RhlE2_{1-434}$ (::3xFLAG-$E2_{1-}$
807 $_{434}$) and 3xFLAG-tagged $RhlE2_{K51A}$ (::3xFLAG-$E2_{K51A}$). Strains background is indicated, and
808 experimental details are described in Materials and Methods. At least three independent biological
809 replicates were tested, results from a representative plate is shown.

810

811 **Figure 3. Role of RhlE1 and RhlE2 in *P. aeruginosa* motilities and biofilm formation. (A)** Surface
812 area covered by the swimming, swarming and twitching wild type PAO1 (WT, black diamonds), the
813 Δ*rhlE1* mutant (ΔE1,dark grey triangles), the Δ*rhlE2* mutant (ΔE2, light grey circles) and the
814 Δ*rhlE1*Δ*rhlE2* mutant (ΔE1ΔE2, white squares) cells (± standard deviation) as calculated by averaging
815 data from four individual plates. **(B)** Surface attached biomass, measured by crystal violet staining, of
816 wild type PAO1 and *rhlE1/rhlE2* mutant strains after 6 hours (attachment phase) or 12 hours (biofilm
817 formation) of growth at 37°C in 24-microtiter plates. **(C)** Complementation of swarming motility using

818 mini-Tn7 constructs carrying 3xFLAG-tagged RhlE1 (::3xFLAG-E1), 3xFLAG-tagged RhlE2
819 (::3xFLAG-E2) expressed in a Δ*rhlE1*Δ*rhlE2* mutant Each value is the average of three different
820 cultures ± standard deviation. (*, $p < 0.05$; **, $p < 0.01$)
821
822 **Figure 4. The RhlE2 regulon. (A)** Example of wild type PAO1, Δ*rhlE1* mutant, Δ*rhlE2* mutant and
823 the Δ*rhlE1*Δ*rhlE2* mutant swarming cells that were subjected to RNA-sequencing analysis. **(B)** Volcano
824 plot representation of transcriptome comparison between the wild type PAO1 (WT) and Δ*rhlE1* (ΔE1)
825 or Δ*rhlE2* (ΔE2) or Δ*rhlE1*Δ*rhlE2* (ΔE1ΔE2). The genes are colored black if they pass the thresholds
826 for −log10 P value (P value < 0.05) and log fold change |FC| ≥2. **(C)** Relative transcript abundance in
827 the wild type PAO1 and *rhlE1/rhlE2* mutant strains as determined by RT-qPCR (RT-qPCR fold
828 change). Values are represented as averages of 3 independent replicates for every strain. **(D)** Cell
829 density-dependent β-galactosidase expression of a transcriptional/translational *lasB'-'lacZ* fusion
830 carried by plasmid pTS400 (39) in wild type PAO1 (black bars), Δ*rhlE1* mutant (ΔE1,dark grey bars),
831 Δ*rhlE2* mutant (ΔE2, light grey bars) and Δ*rhlE1*Δ*rhlE2* mutant (ΔE1ΔE2, white bars). Each value is
832 the average of three different cultures ± standard deviation.
833
834 **Figure 5. RhlE2 regulation of *P. aeruginosa* virulence. (A)** Elastase activity and **(B)** pyocyanin levels
835 of wild type PAO1 (black bars), Δ*rhlE1* mutant (ΔE1, dark grey bars), Δ*rhlE2* mutant (ΔE2, light grey
836 bars) and Δ*rhlE1*Δ*rhlE2* mutant (ΔE1ΔE2, white bars) supernatant. **(C)** Survival curves of *G.*
837 *mellonella* larvae infected with wild type PAO1 and *rhlE1/rhlE2* mutant strains. PBS, larvae injected
838 with sterile physiological solution. Each experiment (A-C) was repeated at least with three different
839 independent cultures for each strain, values indicated average from biological replicates ± standard
840 deviation. For experimental details see Material and Methods.
841
842 **Figure 6. ATPase activity of recombinant RhlE1 and RhlE2. (A)** RhlE proteins purification.
843 Aliquots (2.5 µg) of the nickel-agarose preparations of wild type (WT) RhlE1(lane 1), and mutant K51A
844 (lane 2), wild type (WT) RhlE2 (lane 3), and mutant K51A (lane 4) were analyzed by SDS-PAGE. The

845 polypeptides were visualized by staining with Coomassie Blue dye. The positions and sizes (kDa) of
846 marker polypeptides are indicated on the left. **(B)** RhlE proteins ATPase activity. Reaction mixtures (15
847 µl) containing 50 mM Tris-HCl (pH 8.0), 5 mM DTT, 2 mM MgCl2, 1 mM [γ-^{32}P] ATP, 250 ng/µl
848 Poly(U) (or no RNA; empty symbol), and enzyme as specified were incubated for 15 min at 37 °C. Pi
849 release was determined as described in Materials and Methods and was plotted as a function of input
850 protein. **(C)** RhlE proteins catalytic mutants. Reaction mixtures (15 µl) containing 50 mM Tris-HCl
851 (pH 8.0), 5 mM DTT, 2 mM MgCl2, 1 mM [γ-^{32}P] ATP, 250 ng/µl Poly(U), and 100 ng/µl of enzyme
852 as specified were incubated for 15 min at 37 °C. The extends of ATP hydrolysis are plotted. **(D)** ATPase
853 activity and RNA length. Reaction mixtures (15 µl) 50 mM Tris-HCl (pH 8.0), 5 mM DTT, 2 mM
854 MgCl2, 1 mM [γ-^{32}P] ATP, 2 µM polyribouridylic acid (either U41, U26, U16 or U10) as specified,
855 and 50 ng/µl of RhlEs were incubated for 15 min at 37 °C. The extends of ATP hydrolysis are plotted.
856 **(E)** RNA hairpin recognition. Reaction mixtures (15 µl) 50 mM Tris-HCl (pH 8.0), 5 mM DTT, 2 mM
857 MgCl2, 1 mM [γ-^{32}P] ATP, 2 µM of an oligoribonucleotide as specified and 50 ng/µl of RhlEs were
858 incubated for 15 min at 37 °C. The extends of ATP hydrolysis are plotted. **(F)** Recognition of structured
859 RNA. Reaction mixtures (15 µl) 50 mM Tris-HCl (pH 8.0), 5 mM DTT, 2 mM MgCl2, 1 mM [γ-^{32}P]
860 ATP, 80 ng/µl MS2 or 100 ng/µl *E. Coli* rRNA of and 50 ng/µl of RhlEs were incubated for 15 min at
861 37 °C. The extends of ATP hydrolysis are plotted. (B-F) Data are the average ± SEMs from three
862 independent experiments.
863
864 **Figure 7. Complementation assays with RhlE2 variants. (A)** Swarming motility and **(B)** *lasB'-'lacZ*
865 expression of wild type PAO1, Δ*rhlE2* mutant (ΔE2) and Δ*rhlE2* mutant carrying a mini-Tn7 construct
866 expressing either 3xFLAG-tagged RhlE2 (::3xFLAG-E2) or 3xFLAG-tagged RhlE2$_{1-434}$ (::3xFLAG-
867 E2$_{1-434}$), or 3xFLAG-tagged RhlE2$_{K51A}$ (::3xFLAG-E2$_{K51A}$). Each experiment was repeated at least with
868 three different independent cultures for each strain, values indicated average from biological replicates
869 ± standard deviation. For experimental details see Material and Methods.
870
871 **Figure 8. RhlE2 - RNase E interaction.** Pull-down assays of 3xFLAG-RhlE2**,** 3xFLAG-tagged

872 RhlE2$_{1-434}$ and 3xFLAG-RhlE1 and SDS-page analysis of co-eluting proteins. Culture of **(A)** Δ*rhlE2*
873 mutant carrying a mini-Tn7 construct expressing either 3xFLAG-tagged RhlE2 (3xFLAG-RhlE2) or
874 RhlE2 (untagged RhlE2) or of **(B)** Δ*rhlE2* mutant carrying a mini-Tn7 construct expressing 3xFLAG-
875 tagged RhlE2$_{1-434}$ (3xFLAG-RhlE2$_{1-434}$) and Δ*rhlE1* mutant carrying a mini-Tn7 construct expressing
876 3xFLAG-tagged RhlE1 (3xFLAG-RhlE1) were grown on NYB with 0.05% arabinose at 37°C up to
877 idiophase of growth (O.D. ~1.8). Arrowheads proteins were identified by mass-spectrometry. Other
878 proteins co-eluting with 3xFLAG-RhlE2 were identified by mass-spectrometry and comparison of
879 normalized peptide counts present in the untagged RhlE2 sample, as shown in panel A. **(C)**
880 Quantification of top three proteins which peptides were significantly enriched in 3xFLAG-RhlE2,
881 meaning RNase E, PNPase and RNase R as compared to other strains. Pull-down of 3xFLAG-RhlE2
882 was performed in triplicates (1, 2 and 3), as well in absence (no RNase) and presence (RNase) of RNase
883 A treatment. **(D)** Reconstitution of adenylate cyclase in the *E. coli* strain BTH101 using a bacterial two-
884 hybrid approach was detected by red colour of colonies due to media acidification derived from maltose
885 fermentation when colonies were grown on McConkey plates containing 1% maltose, 0.5 mM IPTG,
886 100 µg/ml ampicillin, and 50 µg/ml chloramphenicol agar plates, as shown). The interactions were also
887 quantified in Miller Units by β-galactosidase assays using liquid cultures of the same strains. Each value
888 is the average of three different cultures ± standard deviation (*, $p < 0.05$; **, $p < 0.01$).
889
890 **Figure 9**. **ATPase activity of recombinant RhlE2$_{1-434}$. (A)** RhlE2$_{1-434}$ purification. Aliquots (2.5 µg)
891 of the nickel-agarose preparations of RhlE2$_{1-434}$ (lane 1) and double mutant RhlE2$_{1-434,\ K51A}$ (lane 2)
892 were analyzed by SDS-PAGE. The polypeptides were visualized by staining with Coomassie Blue dye.
893 The positions and sizes (kDa) of marker polypeptides are indicated on the left. (B) ATPase. Reaction
894 mixtures (15 µl) containing 50 mM Tris-HCl (pH 8.0), 1 mM DTT, 2 mM MgCl2, 1 mM [γ-^{32}P] ATP,
895 250 ng/µl Poly(U), and 100 ng/µl of RhlE2 (1-434) or K51A mutant were incubated for 15 min at 37
896 °C. The extends of ATP hydrolysis are plotted. **(C)** ATPase. Reaction mixtures (15 µl) containing 50
897 mM Tris-HCl (pH 8.0), 1 mM DTT, 2 mM MgCl2, 1 mM [γ-^{32}P] ATP, 250 ng/µl Poly(U) and RhlE2(1-

898 434) or K51 mutant protein as specified were incubated for 15 min at 37 °C. Pi release was plotted as a
899 function of input protein. **(B-C)** Data are the average ± SEMs from three independent experiments.
900
901 **Figure 10. RhlE2 regulation of RNA stability.** Determination of the steady state levels and half-life
902 of PA1897, PA2314, PA2268 and *lasB* mRNA by RT-qPCR in the wild type PAO1 and Δ*rhlE2* mutant.
903 Strains were grown in NYB medium until they reached an OD_{600} of 1.5. Then 250 µg/ml rifampicin
904 was added and samples after 1, 5, 10, 15 and 20 minutes were collected for RNA extraction and cDNA
905 synthesis. The steady state levels of mRNAs were normalized to *rpoD* and *rplA* mRNA levels. The
906 level of each mRNA levels at t_0 was set to 100% while at t_{20} was set to 0 and relative % of transcript
907 remaining is plotted over time. The results represent the average of two independent experiments
908 including each three technical replicates. The error bars represent SDs.
909

A

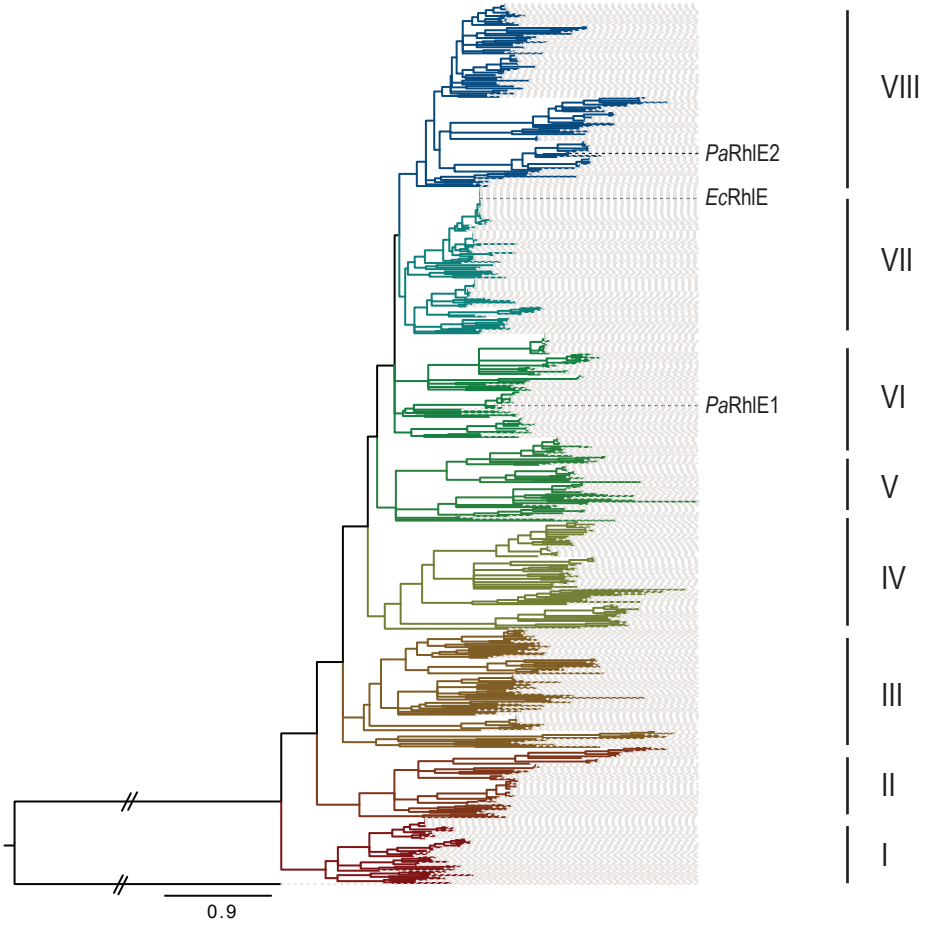
PaRhlE2
EcRhlE
PaRhlE1
VIII
VII
VI
V
IV
III
II
I
0.9

B

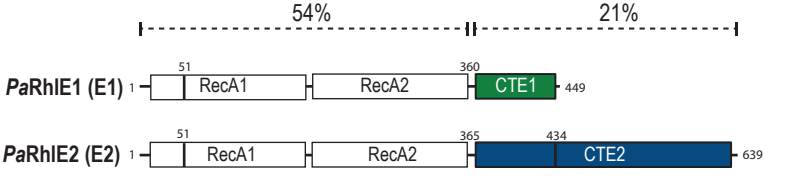
54%
21%
PaRhlE1 (E1)
1
51
RecA1
RecA2
360
CTE1
449
PaRhlE2 (E2)
1
51
RecA1
RecA2
365
434
CTE2
639

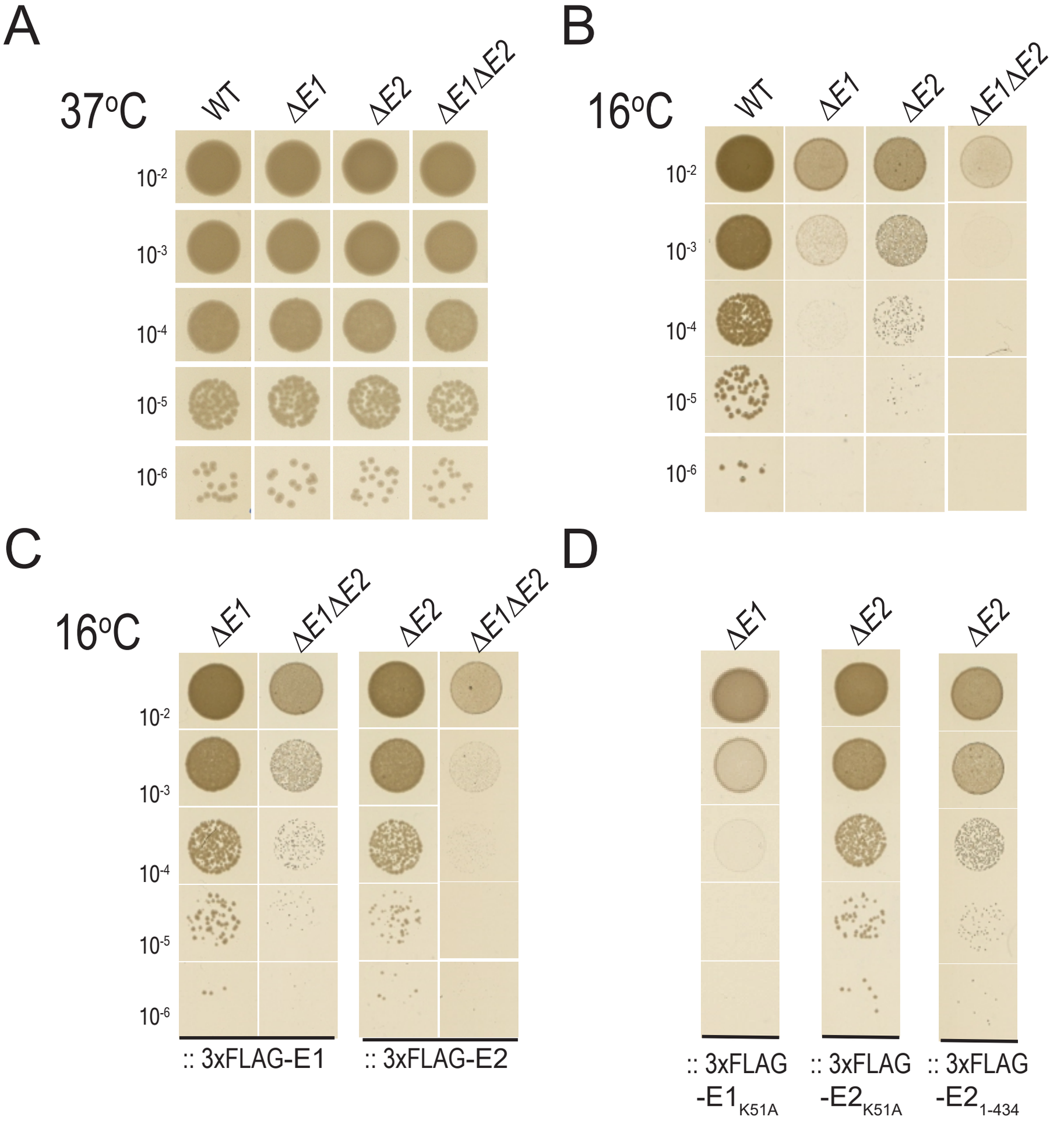
A
37°C
WT
ΔE1
ΔE2
ΔE1ΔE2
10-2
10-3
10-4
10-5
10-6
B
16°C
WT
ΔE1
ΔE2
ΔE1ΔE2
10-2
10-3
10-4
10-5
10-6
C
16°C
ΔE1
ΔE1ΔE2
ΔE2
ΔE1ΔE2
10-2
10-3
10-4
10-5
10-6
:: 3xFLAG-E1
:: 3xFLAG-E2
D
ΔE1
ΔE2
ΔE2
:: 3xFLAG -E1K51A
:: 3xFLAG -E2K51A
:: 3xFLAG -E21-434

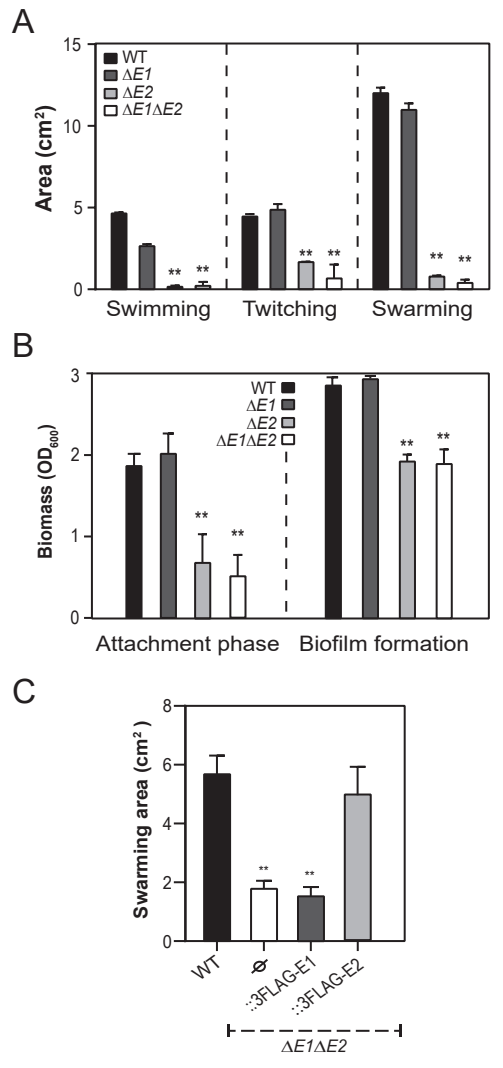
A
Area (cm²)
WT
ΔE1
ΔE2
ΔE1ΔE2
Swimming
Twitching
Swarming
B
Biomass (OD600)
Attachment phase
Biofilm formation
C
Swarming area (cm²)
WT
::3FLAG-E1
::3FLAG-E2
ΔE1ΔE2

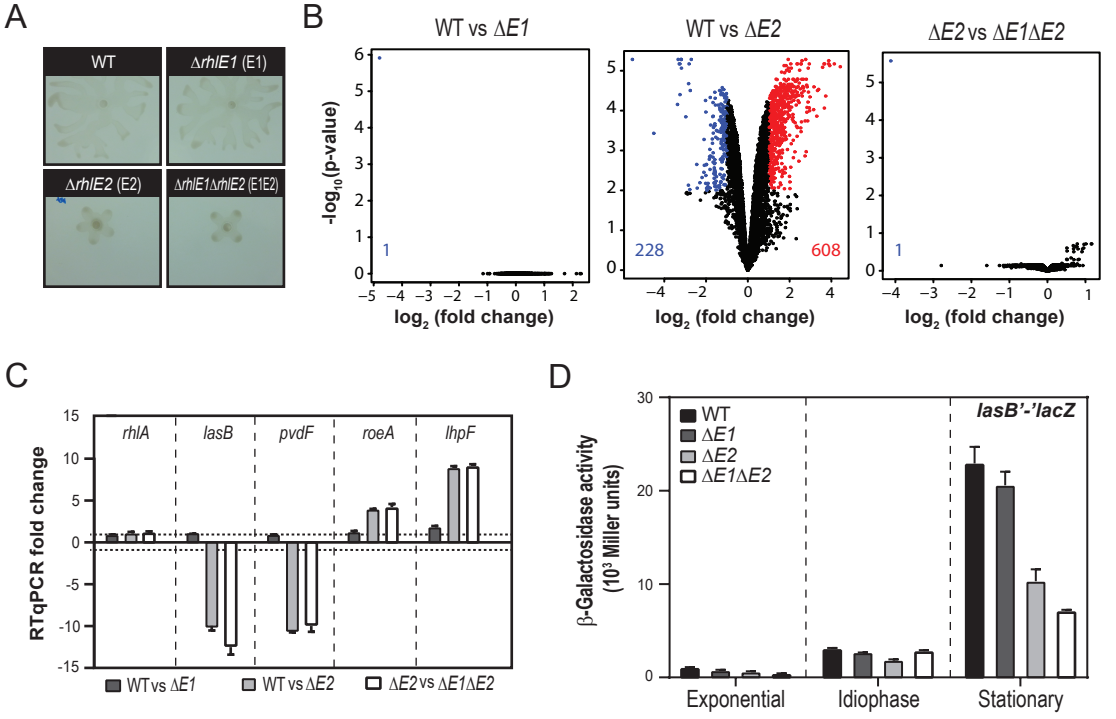
A
WT
ΔrhlE1 (E1)
ΔrhlE2 (E2)
ΔrhlE1ΔrhlE2 (E1E2)
B
WT vs ΔE1
WT vs ΔE2
ΔE2 vs ΔE1ΔE2
-log10 (p-value)
log2 (fold change)
1
228
608
1
C
RTqPCR fold change
rhlA
lasB
pvdF
roeA
lhpF
WT vs ΔE1
WT vs ΔE2
ΔE2 vs ΔE1ΔE2
D
β-Galactosidase activity (10³ Miller units)
lasB'-'lacZ
WT
ΔE1
ΔE2
ΔE1ΔE2
Exponential
Idiophase
Stationary

A

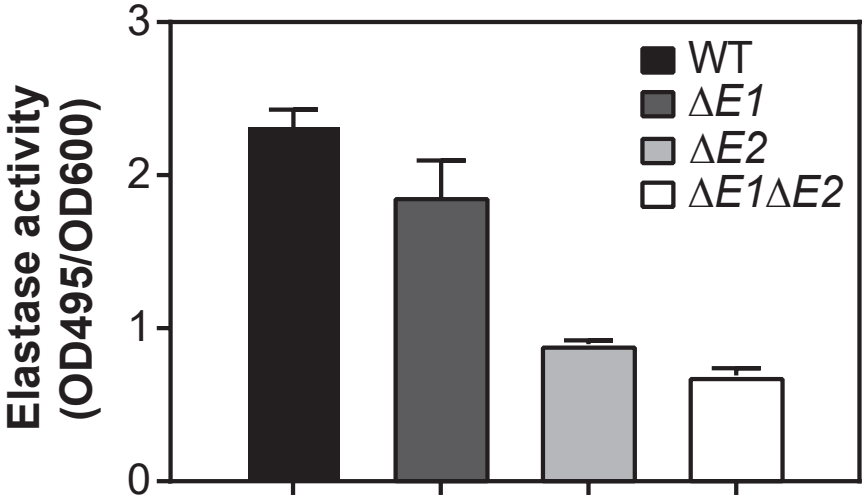
Elastase activity
(OD495/OD600)
3
2
1
0
WT
ΔE1
ΔE2
ΔE1ΔE2

B

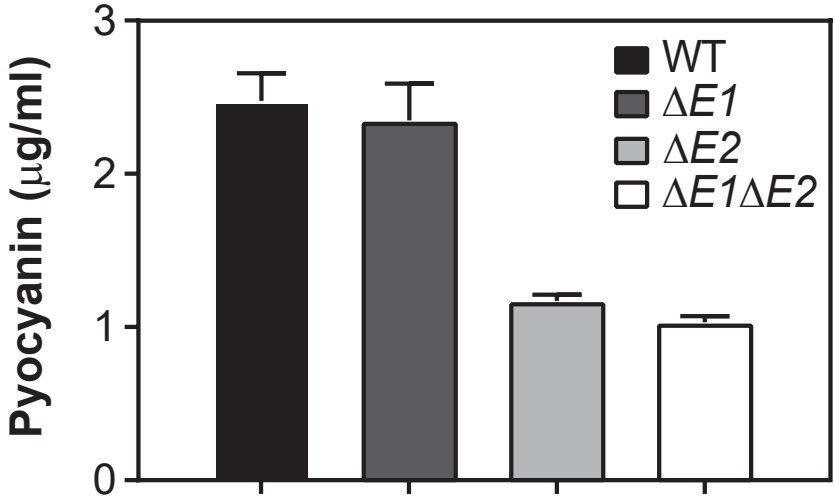
Pyocyanin (μg/ml)
3
2
1
0
WT
ΔE1
ΔE2
ΔE1ΔE2

C

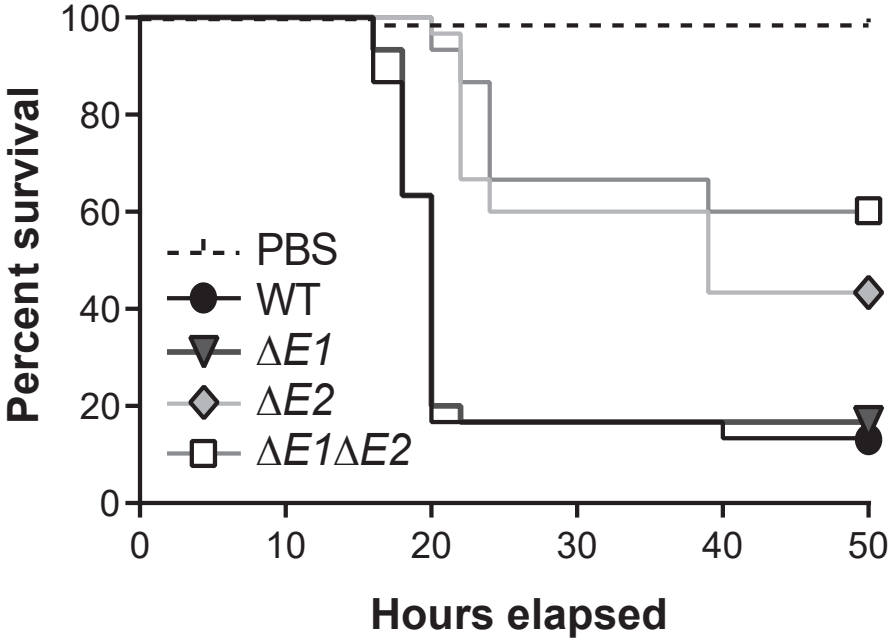
Percent survival
100
80
60
40
20
0
PBS
WT
ΔE1
ΔE2
ΔE1ΔE2
0
10
20
30
40
50
Hours elapsed

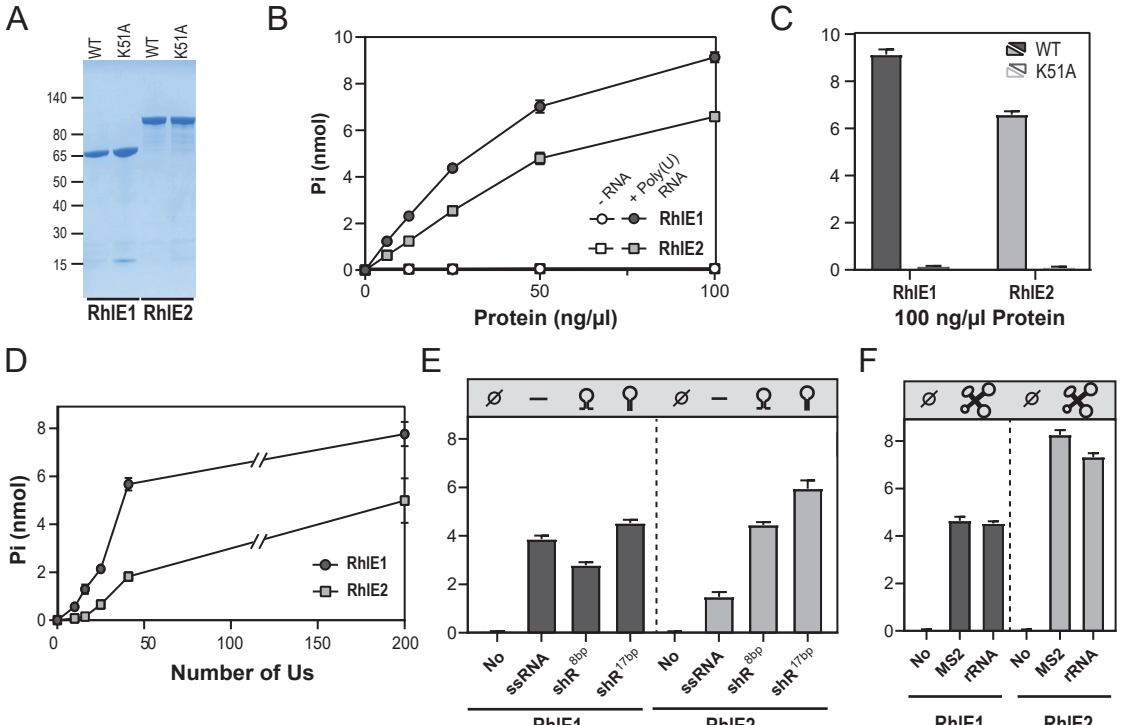
A
WT
K51A
WT
K51A
140
80
65
50
40
30
15
RhlE1 RhlE2
B
Pi (nmol)
Protein (ng/µl)
- RNA
+ Poly(U) RNA
RhlE1
RhlE2
C
WT
K51A
RhlE1
RhlE2
100 ng/µl Protein
D
Pi (nmol)
Number of Us
RhlE1
RhlE2
E
No
ssRNA
shR 8bp
shR 17bp
RhlE1
RhlE2
F
No
MS2
rRNA
RhlE1
RhlE2

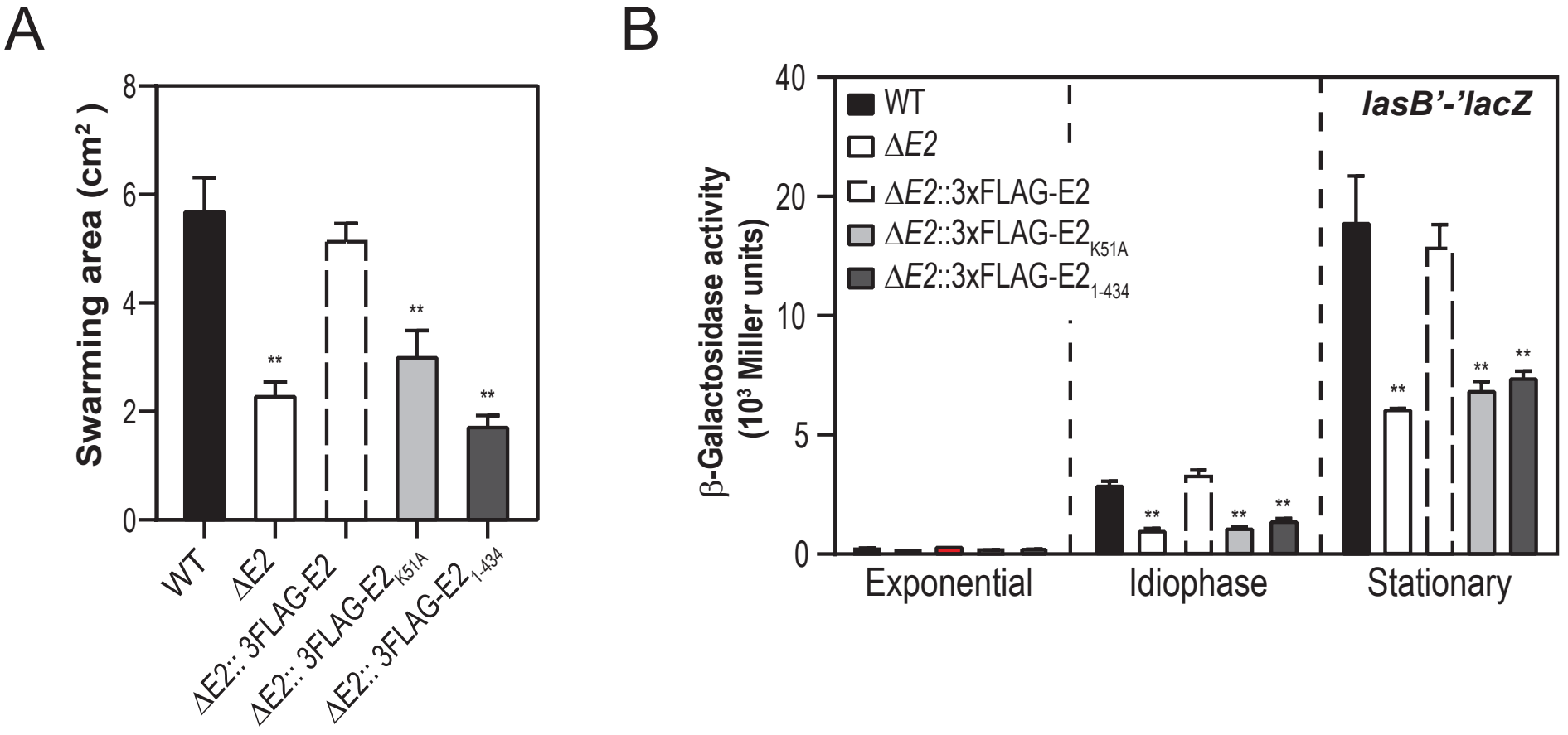
A
Swarming area (cm²)
8
6
4
2
0
**
**
**
WT
ΔE2
ΔE2:: 3FLAG-E2
ΔE2:: 3FLAG-E2K51A
ΔE2:: 3FLAG-E21-434
B
β-Galactosidase activity
(10³ Miller units)
40
20
10
5
0
WT
ΔE2
ΔE2::3xFLAG-E2
ΔE2::3xFLAG-E2K51A
ΔE2::3xFLAG-E21-434
lasB'-'lacZ
**
**
**
**
**
Exponential
Idiophase
Stationary

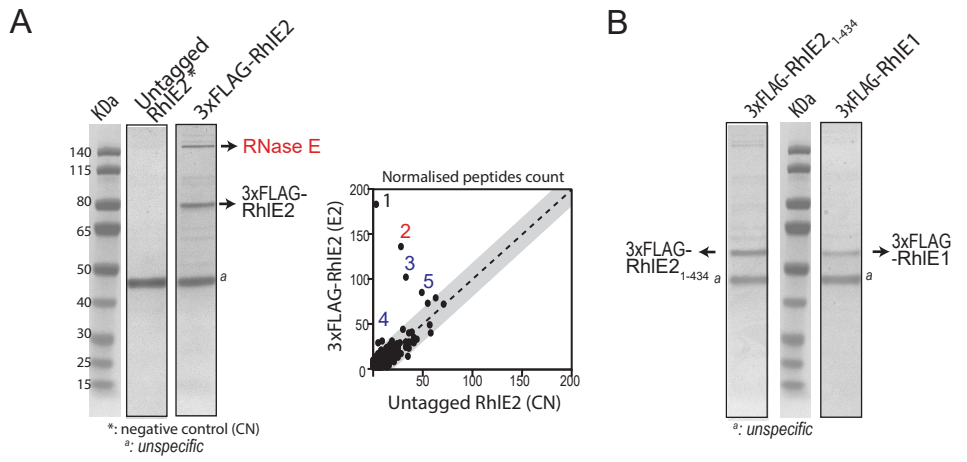

C

Hit		Size (kDa)	1		2		3		3xFLAG-RhlE1	3xFLAG-RhlE2 1-434	3xFLAG-RhlE2	
			CN	E2	CN	E2	CN	E2			No RNAse	RNAse
1	RhlE2	70	3	183	10	153	6	135	16	263	135	185
2	RNAse E	117	28	136	2	124	23	74	28	56	74	22
3	PNPase	75	33	102	2	154	24	52	45	74	52	25
4	RNAse R	100	5	29	12	31	8	25	7	25	13	8
5	DnaK	68	48	85	42	82	32	54	70	78	78	85
	RhlE1	49	0	0	0	0	0	0	293	5	0	0

D

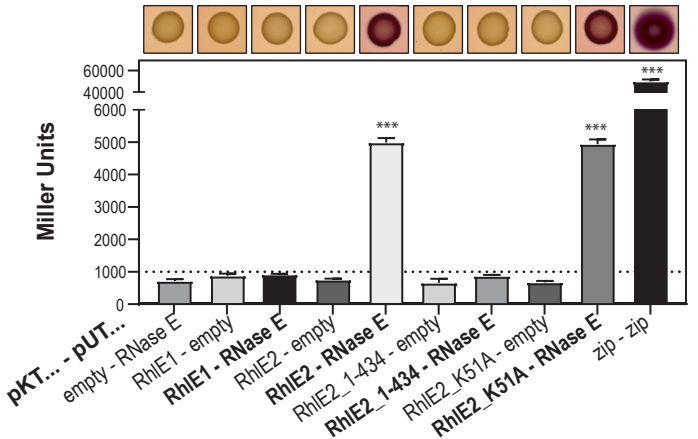

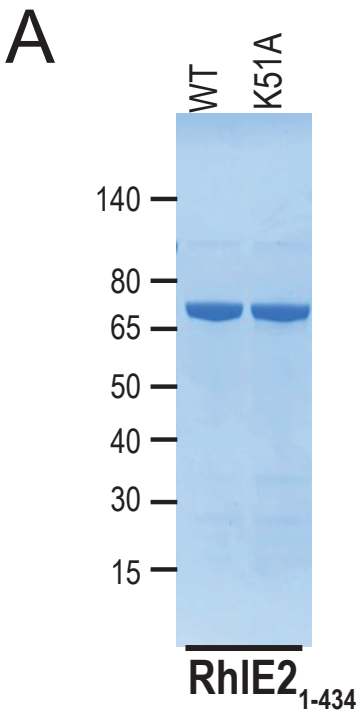
A
WT
K51A
140
80
65
50
40
30
15
RhlE2 1-434

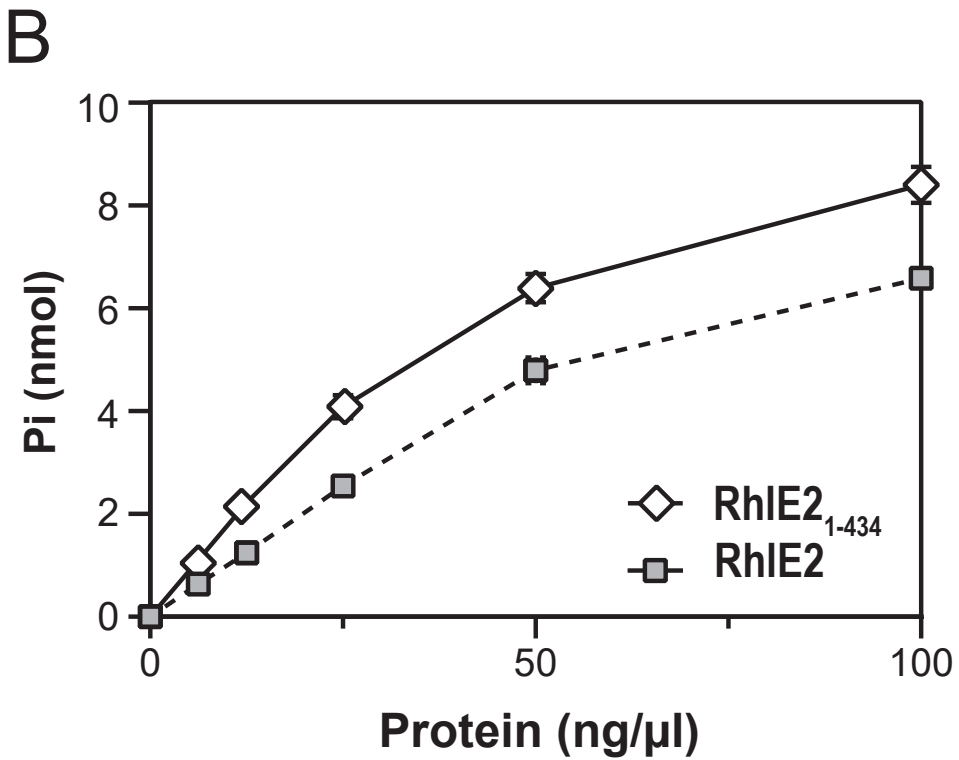
B
Pi (nmol)
10
8
6
4
2
0
0
50
100
Protein (ng/µl)
RhlE2 1-434
RhlE2

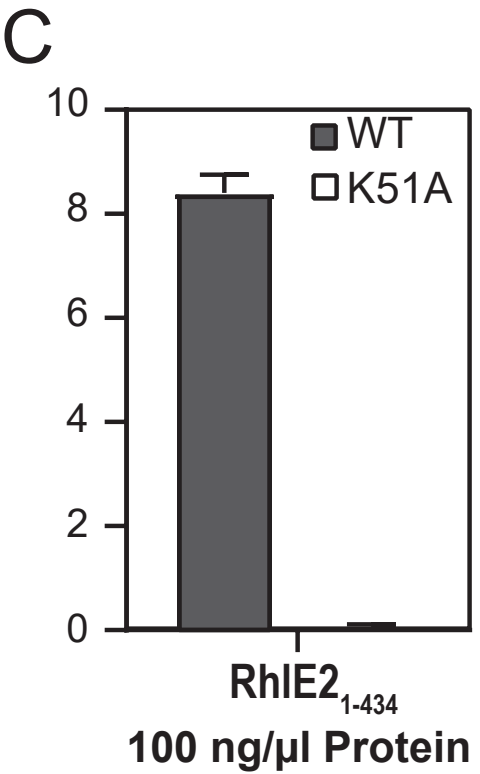
C
10
8
6
4
2
0
WT
K51A
RhlE2 1-434
100 ng/µl Protein

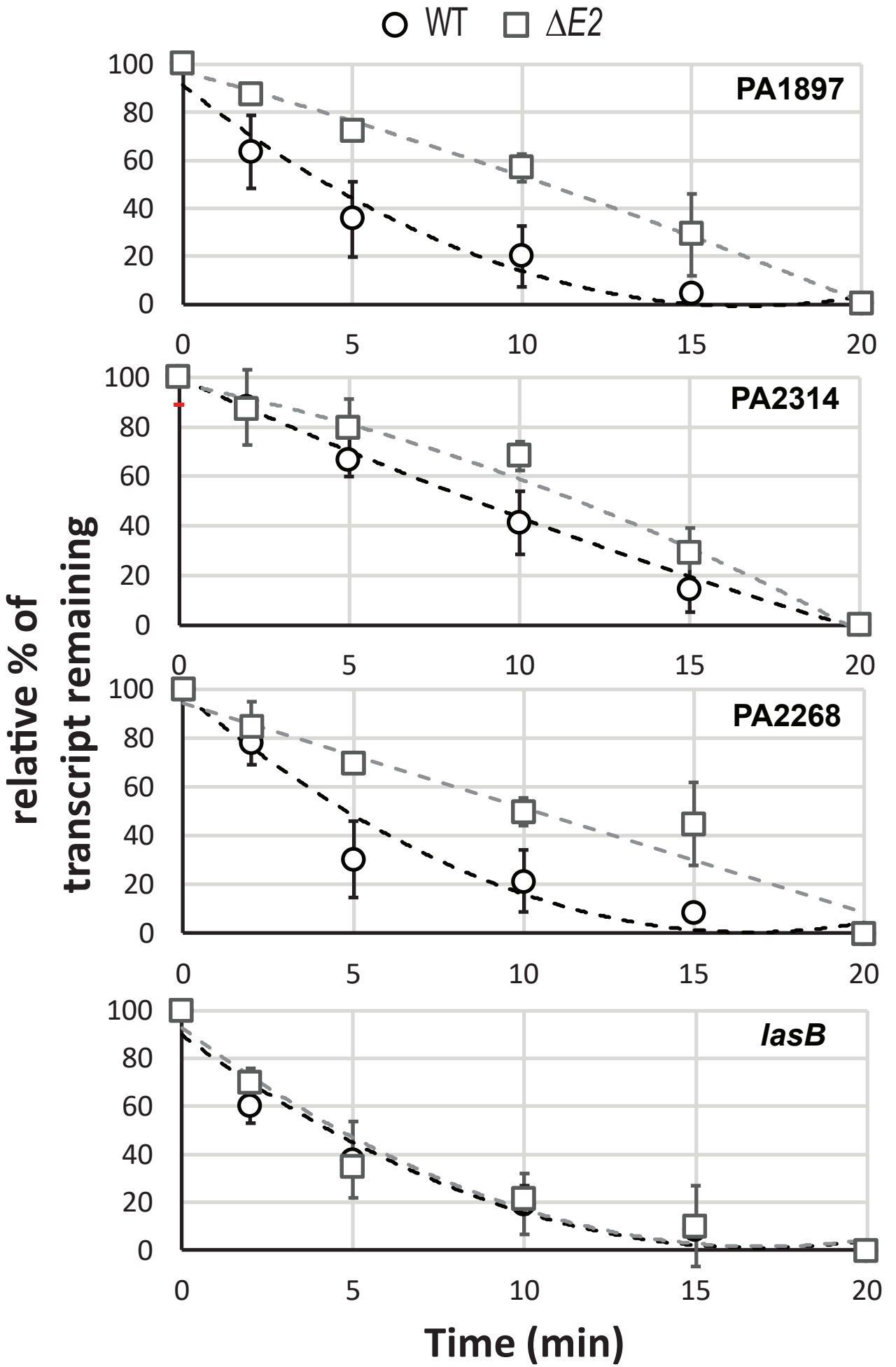
WT
ΔE2
PA1897
PA2314
PA2268
lasB
relative % of transcript remaining
Time (min)
0
20
40
60
80
100
0
5
10
15
20